AD-A037 829 STANFORD RESEARCH INST MENLO PARK CALIF F/G 6/18
INVESTIGATION OF OCULAR EFFECTS OF CHRONIC EXPOSURES OF PRIMATE--ETC(U)
SEP 76 L N HEYNICK, P POLSON, A KARP DAMD17-74-C-4135

UNCLASSIFIED NL

1 OF 1
ADA037829

END

DATE FILMED
4-77

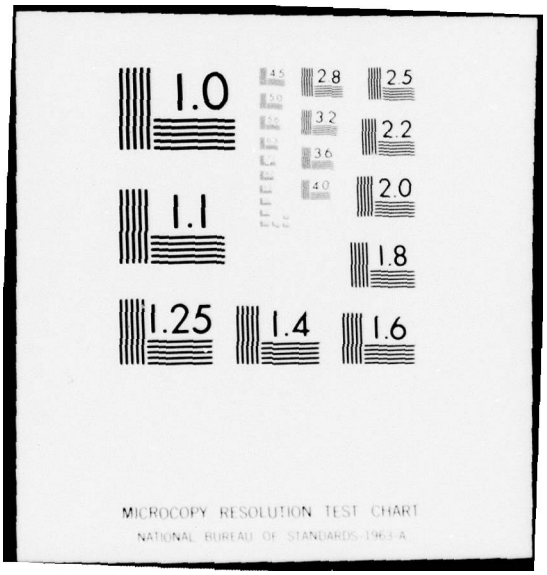
1.0
1.1
1.25
1.4
1.6
1.8
2.0
2.2
2.5
2.8
3.2
3.6
4.0
4.5
5.0
5.6
MICROCOPY RESOLUTION TEST CHART
NATIONAL BUREAU OF STANDARDS-1963-A

(19)

Final Technical Report *September 1976*

INVESTIGATION OF OCULAR EFFECTS OF CHRONIC EXPOSURES OF PRIMATES TO MICROWAVE RADIATION AT 2.45 GHz-- PHASE I

By: L. N. HEYNICK P. POLSON A. KARP

Prepared for:

U.S. ARMY MEDICAL RESEARCH AND DEVELOPMENT COMMAND
WASHINGTON, D.C. 20314
Attention: HQDA (SGRD)

CONTRACT DAMD17-74-C-4135

Approved for public release;
distribution unlimited

STANFORD RESEARCH INSTITUTE
Menlo Park, California 94025 · U.S.A.

STANFORD RESEARCH INSTITUTE
Menlo Park, California 94025 · U.S.A.

Final Technical Report
Covering the Period 29 September 1974 to 30 June 1975

September 1976

INVESTIGATION OF OCULAR EFFECTS OF CHRONIC EXPOSURES OF PRIMATES TO MICROWAVE RADIATION AT 2.45 GHz-- PHASE I

By: L. N. HEYNICK P. POLSON A. KARP

Prepared for:

U.S. ARMY MEDICAL RESEARCH AND DEVELOPMENT COMMAND
WASHINGTON, D.C. 20314
Attention: HQDA (SGRD)

CONTRACT DAMD17-74-C-4135

SRI Project 3572

Approved by:

DAVID A. JOHNSON, *Director*
Radio Physics Laboratory

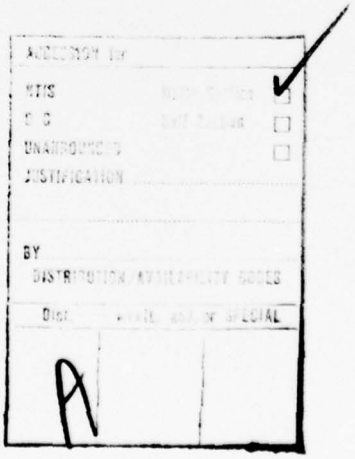

Copy No. 26

SECURITY CLASSIFICATION OF THIS PAGE (When Data Entered)

REPORT DOCUMENTATION PAGE

READ INSTRUCTIONS BEFORE COMPLETING FORM

1. REPORT NUMBER

2. GOVT ACCESSION NO.

3. RECIPIENT'S CATALOG NUMBER

4. TITLE (and Subtitle)
INVESTIGATION OF OCULAR EFFECTS OF CHRONIC EXPOSURES OF PRIMATES TO MICROWAVE RADIATION AT 2.45 GHz, PHASE I.

5. TYPE OF REPORT & PERIOD COVERED
Final Technical Report.
Covering the period 29 September 1974 — 30 June 1975

6. PERFORMING ORG. REPORT NUMBER
SRI Project 3572

7. AUTHOR(s)
Louis N. Heynick Peter Polson Arthur Karp

8. CONTRACT OR GRANT NUMBER(s)
Contract DAMD 17-74-C-4135

9. PERFORMING ORGANIZATION NAME AND ADDRESS
Stanford Research Institute
Menlo Park, California 94025

10. PROGRAM ELEMENT, PROJECT, TASK AREA & WORK UNIT NUMBERS

11. CONTROLLING OFFICE NAME AND ADDRESS
U.S. Army Medical Research and Development Command
Attention: HQDA (SGRD)
Washington, D.C. 20314

12. REPORT DATE
September 1976

13. NO. OF PAGES
59

14. MONITORING AGENCY NAME & ADDRESS (if diff. from Controlling Office)

15. SECURITY CLASS. (of this report)
Unclassified

15a. DECLASSIFICATION/DOWNGRADING SCHEDULE
N/A

16. DISTRIBUTION STATEMENT (of this report)

17. DISTRIBUTION STATEMENT (of the abstract entered in Block 20, if different from report)

18. SUPPLEMENTARY NOTES

19. KEY WORDS (Continue on reverse side if necessary and identify by block number)
Microwave cataracts
Cataractogenesis, Microwave
Nonionizing radiation, biological effects of
Microwave exposure systems
Biological effects of microwaves
Nonhuman primates
Microwave ovens

20. ABSTRACT (Continue on reverse side if necessary and identify by block number)
The development is described of a prototype module for irradiating nonhuman primates of sizes up to and including stumptail macaques at 2.45 GHz for long time periods without constraining the animals (except for cage confinement). This developmental work represents the first phase of an investigation to determine whether eye damage can be caused by chronic, low-level exposure to microwaves. The exposure chamber developed is a 35-inch cubical microwave cavity containing a dielectric cage 26 inches wide, 30 inches high, and 24 inches deep. Waveguide-below-cutoff (radiopaque) windows are provided for viewing and ventilation. A

DD FORM 1 JAN 73 1473
EDITION OF 1 NOV 65 IS OBSOLETE

SECURITY CLASSIFICATION OF THIS PAGE (When Data Entered)

19. KEY WORDS (Continued)

20 ABSTRACT (Continued)

Type 2M53 magnetron and appropriate power supply are used to excite the cavity at 2.45 GHz, and a mode stirrer is used to distribute the input power among various modes and polarizations, thereby providing a substantially isotropic microwave environment for the animal within. A bidirectional coupler having calibrated crystal detectors and metering circuits is used to measure and display forward and reflected RF power values, and a feedback circuit is used to maintain the power level constant at any setting. Containers having various quantities of saline were used as first approximations to the RF losses of monkeys in a number of calorimetric measurements of "whole-body" absorption dose rates as related to: values of net (forward minus reflected) power into the cavity and its contents, container placement within the cavity, and saline water mass. The results indicate that absorption dose rate at any given input power is insensitive to container location (indicative of isotropy) and is inversely related to the water mass. Significant features are also mentioned of 12 modules constructed subsequently for an EPA program involving chronic irradiation of squirrel monkeys, and a series of measurements is summarized on saline-containing dolls irradiated with unidirectionally incident plane waves and within a cavity module, to determine "thermal equivalence" between the two forms of radiation.

CONTENTS

ILLUSTRATIONS

TABLES

I INTRODUCTION

This report describes the work performed on Phase I of a program to investigate the possibility of cataract generation in stumptail macaques by chronic, low-level exposure to electromagnetic radiation at 2.45 GHz.

Present exposure standards for nonionizing electromagnetic radiation imply far-field conditions, i.e., unidirectionally incident plane waves. However, the use of omnidirectionally incident radiation is probably the most practical approach toward investigating the effects of chronic, low-level exposures. With this approach, the difficulties and problems involved in constraining or training experimental animals such as monkeys to face a specific direction for long periods of continuous irradiation (e.g., up to eight hours per session) are avoided. The electromagnetic field within a multimode, mode-stirred microwave cavity large enough to accommodate a suitable monkey cage of low-loss dielectric material and excited (at 2.45 GHz) by a properly coupled, controllable magnetron source should constitute the equivalent of an omnidirectionally incident irradiation source. Accordingly, the objective of Phase I was the design, fabrication, testing, and calibration of a microwave-cavity exposure module for housing a single stumptail macaque, with the module to serve as the prototype for the exposure units to be constructed and used, under Phase II, for carrying out the cataractogenesis investigation.

II SUMMARY

The module developed under Phase I basically consists of a powered multimode, mode-stirred microwave cavity that contains a cage of size consonant with the National Academy of Sciences/National Research Council recommendations for housing single primates weighing up to 15 kg. The cage is constructed of dielectric materials having low loss-tangent values at RF, and is designed to withstand the activities of an unrestrained stumptail macaque. Power at 2.45 GHz is fed into the cavity/cage unit from a magnetron source, and the requisite ancillary components and instrumentation are provided for setting, measuring, and automatically maintaining constant RF power levels.

Initial calibration of the prototype module entailed calorimetric measurements of the energy deposited in cylindrical bottles containing 0.15 N saline water* as first approximations for the RF loads presented by monkeys. The energy measurements were taken for various values of water mass, bottle location within the cavity/cage unit of the module, and surface configuration of the water. The data were normalized to the values of total energy absorbed by the cavity/cage unit and its contents. "Whole-body" absorption dose rates and mean values of the power flux density† through the surface of the water were calculated for the values of net RF power fed into the cavity/cage unit.

---

*"Normal" or "physiological" saline, isotonic with blood (9.4 g of NaCl per liter of water.)

†"Power flux density" is defined herein as the ratio of the rate of energy entering an absorbent body to its surface area, and is henceforth abbreviated to "power density."

This calorimetric work was supplemented with a number of measurements of absorbed dosage and the distribution thereof in macaque carcasses irradiated in the module, using the sectioning techniques developed at the University of Washington (Seattle), in conjunction with scanning infrared thermography. Also, measurements of temperature variation with depth in the eye were attempted on an anesthetized macaque, using a micropipette-thermocouple technique also developed at the University of Washington. For these purposes, the module was transported to the University of Washington, and representatives of the U.S. Air Force, Army, Navy, University of Washington, and SRI participated. Discussion of this supplemental work is not included in this report. Instead, various aspects thereof are being documented separately by the participating Service representatives.

Subsequent to the completion of the work on Phase I, 12 modules incorporating a number of significant design improvements were constructed by SRI as part of Contract 68-02-2248 (SRI Project 4407), entitled "Behavioral and Electroencephalographic Responses of Squirrel Monkeys Exposed in Utero to 2450-MHz Electromagnetic Radiation," with the Environmental Protection Agency (EPA). Calorimetric measurements were performed with these modules, using bottles of saline water having masses approximating those of squirrel monkeys and saline-filled rubber dolls of comparable size. In addition, the dolls were irradiated at various orientations relative to the direction of the electric vector of 2.45-GHz plane waves, using a power source and an anechoic chamber available at SRI. The results of these experiments provided an appropriate form of thermal equivalence* between cavity and plane-wave irradiation levels for this species

---

*It should be noted that, because a cavity provides omnidirectional whole-body irradiation and a unidirectional plane-wave source does not, widely applicable biological equivalence between the two types of irradiation would be difficult to define unambiguously. Definitions of equivalence based on biological endpoints relevant to the purported physiological

of primate. A brief summary of this work is included in this report because we believe that the concept and techniques used can be adapted to other animals, such as the stumptail macaque.

In Section III the development of the prototype module is discussed in detail, including the calorimetric measurements with saline-filled bottles. Also, significant improvements incorporated in the 12 modules produced for the aforementioned EPA program are described where appropriate.

Section IV embodies our conclusions and Section V our recommendations for future work on cataractogenesis.

---

effects under investigation are appropriate if their implementation is practical. However, results involving such definitions should be analyzed critically, because it may be possible, in some cases, to obtain the same biological endpoint by different mechanisms or effects from the two methods of irradiation. Thermal equivalence based on the use of calorimetry with a saline-filled doll was taken to be a reasonable first approximation to biological equivalence for chronic irradiation of fetuses in utero in squirrel monkeys.

III DEVELOPMENTAL WORK

A. Preliminary Microwave Cavity Design and Performance

To obtain basic operational characteristics of a multimode, mode-stirred cavity having dimensions sufficiently large to contain a cage adequate for housing a stumptail macaque, a cavity of preliminary design was constructed and tested, without an internal cage. The shape chosen for this first cavity was cubical, about 33 inches on a side. Figure 1 is a photograph of this cavity. To distribute the microwave power entering the cavity broadly among the various possible modes and polarizations, we decided to feed the power into one corner of the cavity, with that body diagonal of the cube as the symmetry axis.

Most of the tests at low power levels discussed below were performed with an Alfred Model 605-204 Microwave Oscillator and a Hewlett-Packard Model 8410A Network Analyzer, which has a polar impedance (Smith chart) oscilloscope display. Polyethylene bottles containing specified quantities of 0.15 N NaCl were used as RF loads within the cavity.

Two methods of exciting the cavity in the manner described above were tested. The first entailed the use of a coaxially fed E-field probe inserted in the corner in alignment with the body diagonal, and having an insertion length that could be varied (up to about a quarter of a wavelength) for coupling-coefficient or impedance-matching purposes. In the second method a short section of waveguide with its central longitudinal axis aligned with the body diagonal was used in conjunction with a suitable impedance-matching device.

Tests of the coaxial-probe, cavity-excitation method were performed by sweeping the oscillator through a frequency band from 2.40 to 2.50

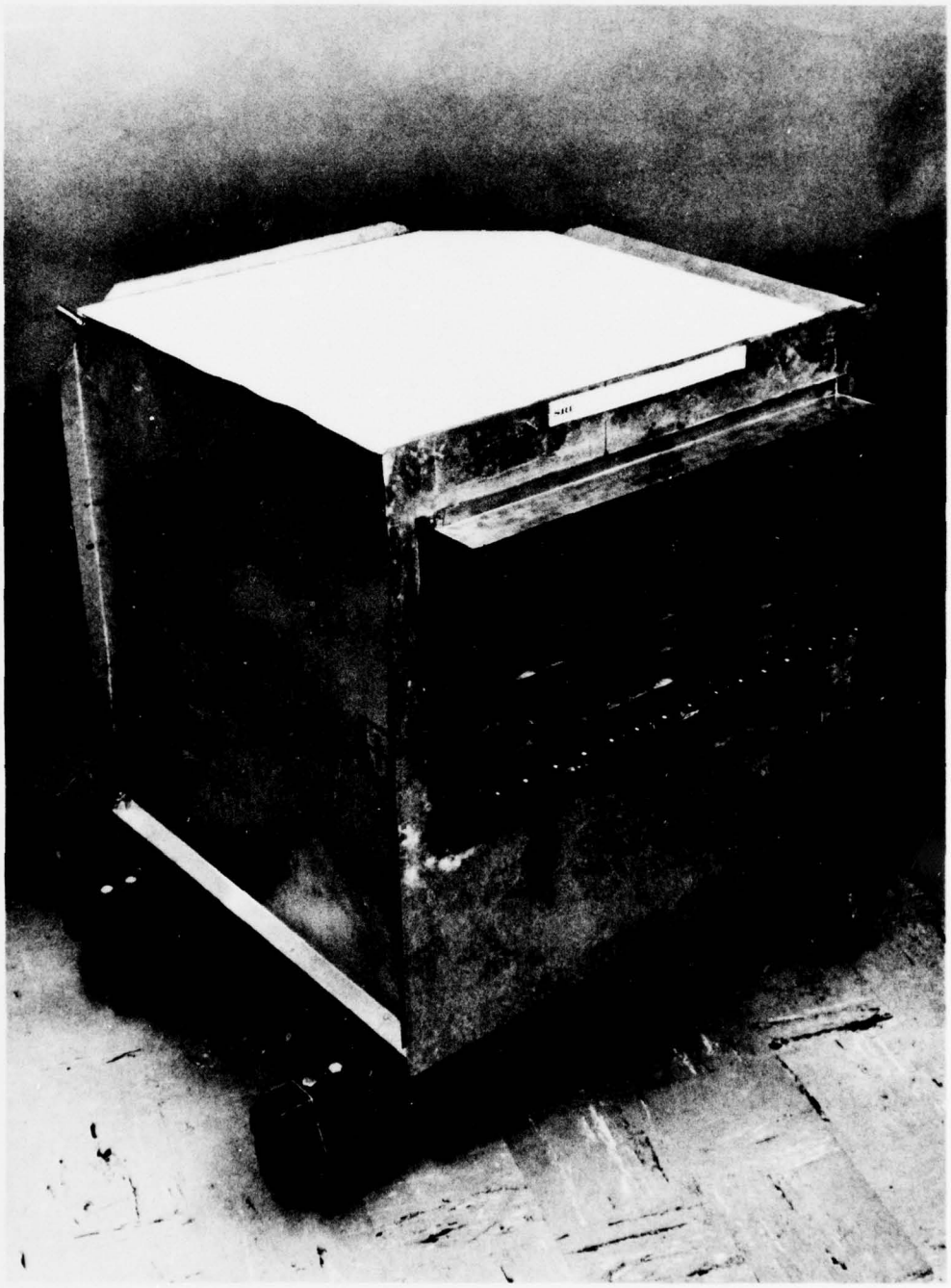

SA-3572-1

FIGURE 1 INITIAL CAVITY

GHz.* The results indicated that the probe could not be adjusted to yield acceptable values of voltage standing-wave ratio (VSWR) unless an auxiliary matching device (e.g., a double-stub tuner) was inserted in the line; even with a double-stub tuner, low VSWR values ($\sim$ 1.1) could be obtained only at a few isolated frequencies, but the "average" VSWR over the band could not be reduced below about 2.0. For the waveguide method of cavity excitation, we decided (for reasons discussed later) to use a waveguide having inner dimensions of 2.84 by 1.34 inches. These dimensions are the same as for Type WR 284 waveguide, which is normally used for the frequency band 2.60-3.95 GHz but is satisfactory for 2.45 GHz because it has a cutoff frequency of 2.08 GHz. For matching purposes, we inserted an E-H tuner in the waveguide at the entrance to the cavity. With this arrangement, we obtained excellent matching--i.e., a maximum VSWR of about 1.2 over the entire band swept. Based on this result, we adopted this method of cavity excitation. (It also appeared possible that the coaxial-probe method of cavity excitation could be improved to obtain satisfactory performance, but this approach was not pursued further.)

Two forms of motor-driven mode-stirrers were tested. The better of the two is shown in Figure 2. Basically, it consists of four 3-by-4 inch rectangles of brass sheet mounted at various angles relative to one another along the periphery of a dielectric disc. A dielectric dowel fastened to the disc (on its axis) serves as the rotation shaft, which is brought through a radiopaque (waveguide-below-cutoff) hole located near the center of one of the side walls of the cavity. An external variable-speed motor coupled to the protruding dielectric shaft is used to rotate the disc. To observe the effects of mode stirring, we loaded the cavity with two

---

*This frequency excursion allows about as many different modes of cavity resonance to be excited as would be at a fixed frequency but with a "good" mode stirrer in operation.

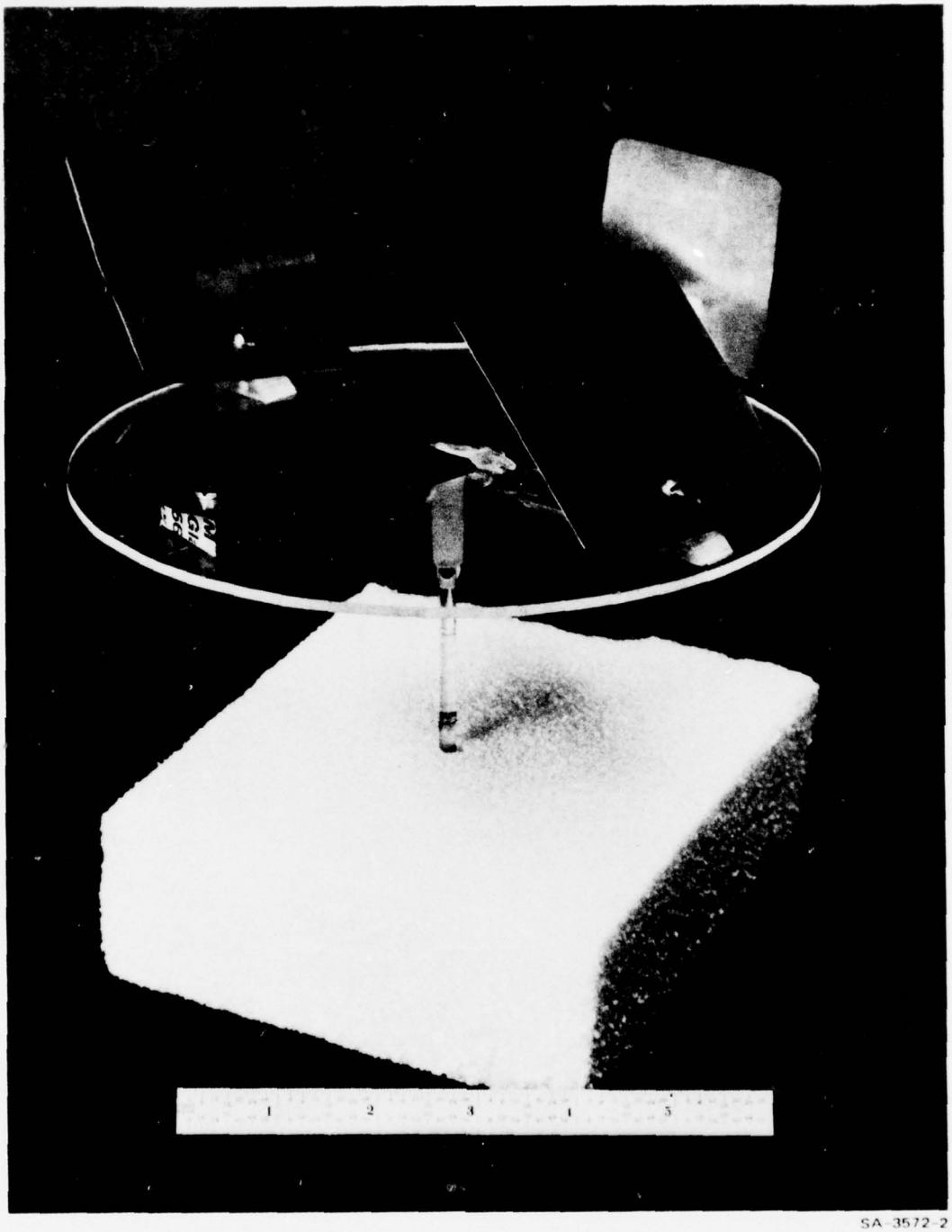

SA-3572-2

FIGURE 2 FOUR-BLADE MODE STIRRER

10-lb bottles of saline water, adjusted the E-H tuner for the lowest maximum VSWR while the cavity was being excited at 2.45 GHz and the mode stirrer was rotating, and photographed the resulting variation of complex input impedance displayed by the Model 8410A Network Analyzer. Figure 3(a) illustrates a typical result. The complicated trajectory traced as a result of the mode-stirrer rotation is a qualitative indication that many modes are successively excited. It is also significant that the entire pattern of complex reflection coefficient lies within a circle corresponding to a VSWR of about 1.3. At this point, we decided to perform a preliminary experiment to determine qualitatively the effects of redistributing the saline water load within the cavity. For this purpose, we attached a string to one of the two bottles, passed the string through a small hole in the top of the cavity, and photographed the impedance pattern obtained while the bottle was being raised to the top of the cavity. This was done with the setting of the E-H tuner unchanged and the mode stirrer rotating as before. The resulting pattern is shown in Figure 3(b). Although the pattern is far more complicated, most significant is the fact that the pattern is largely confined within the circle corresponding to a VSWR of about 1.5.

Because E-H tuners are relatively expensive, we investigated several simpler forms of adjustable matching device. One such device consisted of a sliding inductive iris in close proximity (i.e., virtually coplanar) with a similar capacitive iris, both of which could be adjusted independently. This device operated well but would have required additional developmental work to ensure freedom from arcing at points of poor RF contact. Another device considered was the adjustable iris formed by laterally translating one section of waveguide, relative to an adjacent section, in a direction parallel to the broad walls for inductive tuning and parallel to the narrow walls for capacitive tuning. This type of device was not evaluated because an even simpler form of adjustable iris

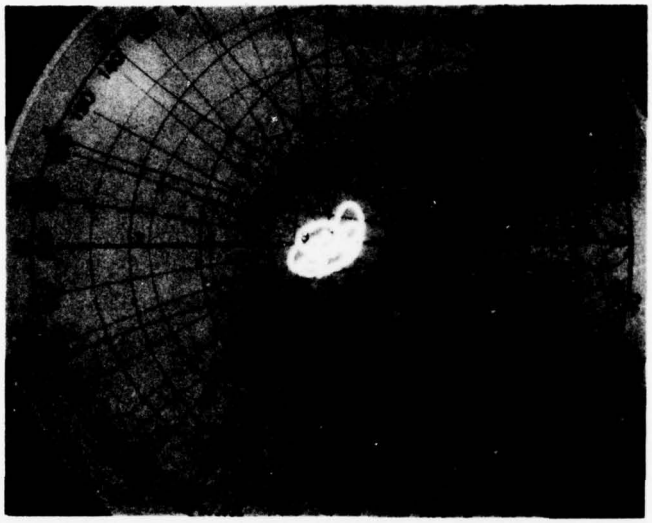

(a) WITH SALINE WATER LOAD IN FIXED LOCATION WITHIN CAVITY

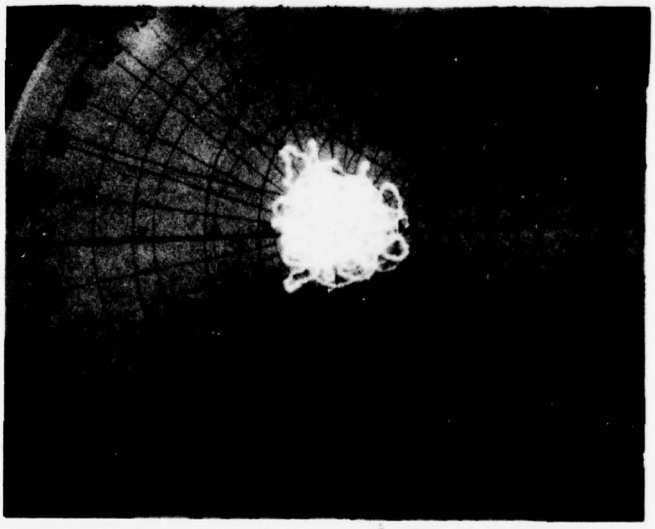

(b) WHILE REDISTRIBUTING SALINE WATER LOAD

SA-3572-3

FIGURE 3 POLAR PATTERNS OF COMPLEX IMPEDANCE OF CAVITY AT 2.45 GHz

proved satisfactory and was adopted. In the latter device, adjustment is effected by rotating one section of waveguide relative to an adjacent section about their common central longitudinal axis. Unlike the previously mentioned devices, the rotational device has only one adjustable parameter, the relative angular displacement. However, adequate matching is achieved within its angular adjustment range. The structure of this iris is shown schematically in Figure 4. The adjustable part, Figure 4(a), is of 1/16-inch-thick brass sheet and has the requisite 2.84-by-1.34-inch waveguide opening. This part is interposed between the triangular flat section, Figure 4(b), and the external waveguide feedline. The flat section has a 3-1/2-inch-diameter hole (i.e., larger than the diagonal of the waveguide opening) and a concentric array of 16 screw holes for mounting the waveguide line at any given fixed orientation while permitting rotation of the adjustable part to provide the required iris opening. The mounting screws also serve as perimeter guides during rotation.

This first cavity was also used to investigate a number of other properties at power levels comparable with or higher than those to be used for monkey irradiation. For convenience in performing such tests, we used a Gerling Moore, Inc., Model 4003/4006 Microwave Power Source available at SRI, capable of yielding 0 to 2.5 kW at 2450 ± 50 MHz. This system is also equipped with the requisite bidirectional coupler and ancillary instrumentation for measuring forward and reflected power, and other accessories such as a water-cooled load. A distinctive feature of this system is the use of WR 284 waveguide dimensions (2.84 by 1.34 inches) for all its microwave components, whereas the standard waveguide types for 2.45 GHz are WR 340 (3.40 by 1.70 inches) and WR 430 (4.30 by 2.15 inches). In addition to the larger physical sizes (and hence higher costs) of WR 340 and WR 430, components such as bidirectional couplers having the required power-handling capabilities ($\sim$ 1 kW) were unobtainable, presumably because the commercial market for such devices is negligible. Accordingly, we decided to work with the WR 284 dimensions.

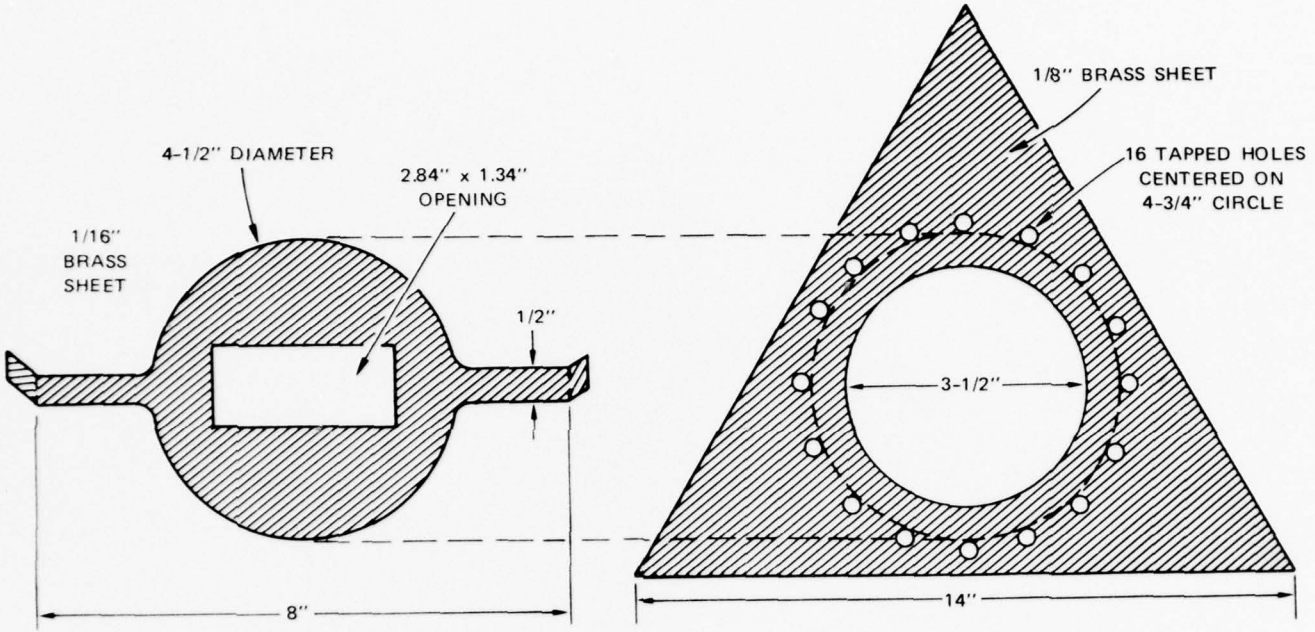

FIGURE 4 SCHEMATIC OF ROTATIONALLY ADJUSTABLE IRIS

A preliminary design of a radiopaque viewing and ventilation window was tested. We replaced a 14-by-30-inch area of the front wall of the cavity with a brass grille of 2-inch squares having a depth of 3 inches (see Figure 1). With several watts of power flowing into the cavity, we used a Narda Model 8300 omnidirectional power-density probe to measure the power density just outside the window and just within the cavity by passing the handle of the probe outward through one of the grille holes. The window attenuation (ratio of internal to external power densities) was found to be about 24 dB. This value would probably be satisfactory. However, as indicated later, we decided to adopt for the prototype a grille size consisting of 1-inch squares, 1-1/2 inches deep, having an attenuation of about 37 dB.

B. Cavity/Cage Unit

1. Cavity, Mode Stirrer, and Iris

In designing the prototype unit, the cubical form of cavity was retained, but the sides were increased from 33 to 35 inches (internally) to accommodate the cage readily and to provide adequate room for the mode stirrer and for the use of a triangular flat section (Figure 4) at the microwave-feed corner. Figure 5 is an internal view of the prototype cavity, showing the mode stirrer, the previously mentioned rotationally adjustable iris at the mouth of the waveguide opening, and the dielectric tray for animal waste collection. The walls of the prototype cavity were fabricated from galvanized-iron sheet. However, it proved more economical to form the 12 EPA cavities by welding together stainless-steel sheets of proper sizes.

Also seen in Figure 5 are the radiopaque windows provided in the door and top panel of the cavity. These windows are of 1-inch-square, 1-1/2-inch-deep grille (of brass in the prototype and of aluminum in the

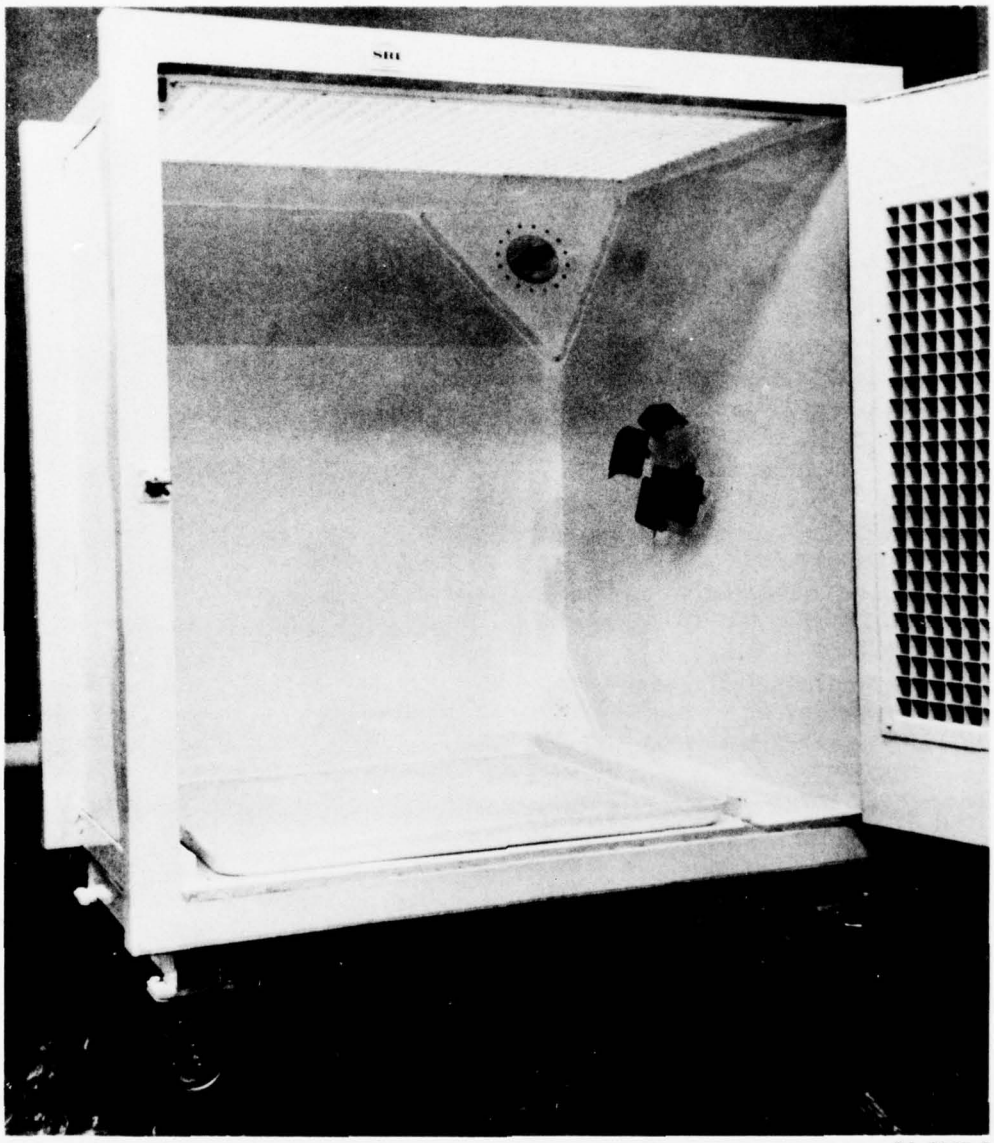

SA-3572-5

FIGURE 5 MICROWAVE CAVITY, WITH DOOR OPEN, SHOWING MODE STIRRER, IRIS, RADIOPAQUE WINDOWS, AND WASTE-COLLECTION TRAY

EPA modules), occupying areas 30 inches wide by 24 inches high in the door and 30 by 18 inches in the top panel. The reduction in the grille size (from 2-inch squares in the initial cavity) ensures that the monkey will not be able to poke its arm through any opening; the new size also provides about 37 dB of attenuation. The door is hinged. Beryllium-copper finger stock was used initially along its periphery to ensure good RF contact when the door is closed. However, when several fingers had broken off through frequent use of the door, it was decided to replace the finger stock with a suitably designed RF choke mounted along the entire perimeter of the cavity opening and to use a pair of toggle clamps to ensure tight closing of the door. After these modifications, RF leakage at the door seal was negligible with powers in excess of 1 kW fed into the cavity. Additional modifications to the door seal, primarily in the design of the RF choke configuration to permit easier fabrication, were used in the EPA modules.

2. Dielectric Cage

The dielectric cage consists of a rectangular box internally about 26 inches wide, 30 inches tall, and 24 inches deep, on legs about 2 inches high. Figure 6 is a photograph of this cage. The front and top panels of the box are of "Fibergrate,"* a polyester-resin/fiberglass material in grille form having cell dimensions of 1 by 4 inches and about 1 inch deep. These panels provide adequate viewing, illumination, and ventilation capabilities (in conjunction with appropriately designed radiopaque windows in the corresponding cavity walls). The bottom panel of the box has this same grille construction, primarily to permit the passage of wastes to the removable dielectric tray placed underneath the cage.

*Manufactured by Fibergrate Corp., P.O. Box 34044, Dallas, Texas 75234.

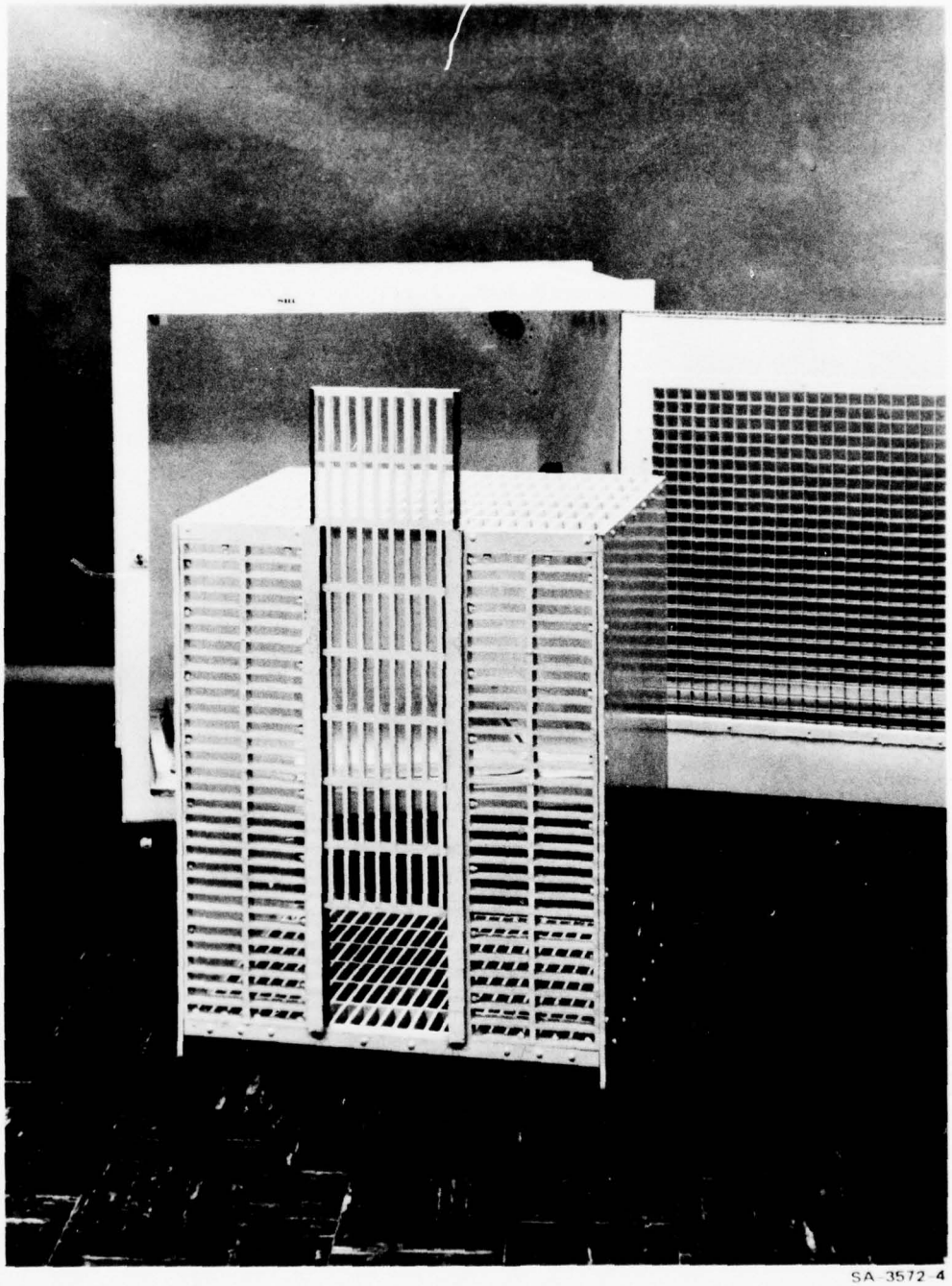

FIGURE 6 DIELECTRIC CAGE

The front panel has a centrally located door (of the same grille material, about 8 inches wide and of full cage height) that can be raised along a pair of dielectric slide brackets to permit transfers of the monkey for eye examinations or to and from a holding cage during periodic cleaning and sterilization of the cavity and cage. The door was designed in this manner so that the cage cannot be opened (by monkey or human) unless the cage is pulled forward partially out of the cavity, thereby permitting the holding cage to be brought flush against the front of the dielectric cage for the transfer.

The Fibergrate material was chosen for the structural members described above because of its excellent mechanical strength, immediate availability in grille form at relatively low cost, and low RF-loss characteristics. It was selected after we had performed rapid semiquantitative tests of the RF absorption characteristics of various candidate materials.

The rear and two side panels of the cage are optically opaque sheets, made originally of polyvinyl chloride (PVC) but now of painted lucite. Lucite was chosen because, in preliminary cage tests within the cavity, the PVC tended to warm up when the cavity was driven at high power levels (e.g., $\sim$ 1 kW) for short time periods (five to ten minutes), indicating that the RF loss tangent of PVC may be too high for a cage to be used for chronic irradiation.

Two cylindrical bars of lucite were installed horizontally across the cage as perches.

No provision was made for feeding solid food to the monkey during RF exposure; such food is to be provided between irradiation periods, using standard metal trays hung on the front part of the cage (with the cavity door open). Apparatus for animal access to liquids (water or Tang) during irradiation (as well as between irradiation periods) was developed. The

liquid is dispensed, from a bottle supported outside the cavity, through low-RF-loss tubing to a small lucite dish mounted within the cage. Several arrangements for controlling the flow rates were devised and tested. We adopted the use of a timing circuit that actuates a solenoid valve for adjustable predetermined periods so as to periodically dispense appropriate increments of liquid. The solenoid is encased in acoustic insulation to dampen the clicks caused by its actuation. When occupancy of the cavity/cage unit by a stumptail macaque (without microwave power) revealed the need to drain excess urine and spilled water from the floor of the cavity, one of several simple methods for doing so was implemented.

Nylon screws were used to assemble the cage and to mount any other structural or functional components within the cavity (such as the slides for the cage door, the lucite perch bars, and the drinking trough).

Figure 7 shows the cage set into the cavity. To slide the cage door open, the cage is pulled forward until the door clears the top of the perimeter of the cavity.

To conserve laboratory floor space, the improved modules for the EPA project were designed for vertical stacking in pairs. A typical pair of modules is shown in Figure 8. Also, each cage was divided into two equal compartments to permit irradiation of two squirrel monkeys concurrently in each unit. An opaque (painted) lucite sheet was installed vertically, extending from front to rear for this purpose, and the central door of the cage was replaced with a pair of similar doors, one on each side of the central partition.

C. Microwave Power Components

1. Magnetron and Power Supply

To perform exposures at various power levels as well as to permit feedback control at any given power level, a microwave source was

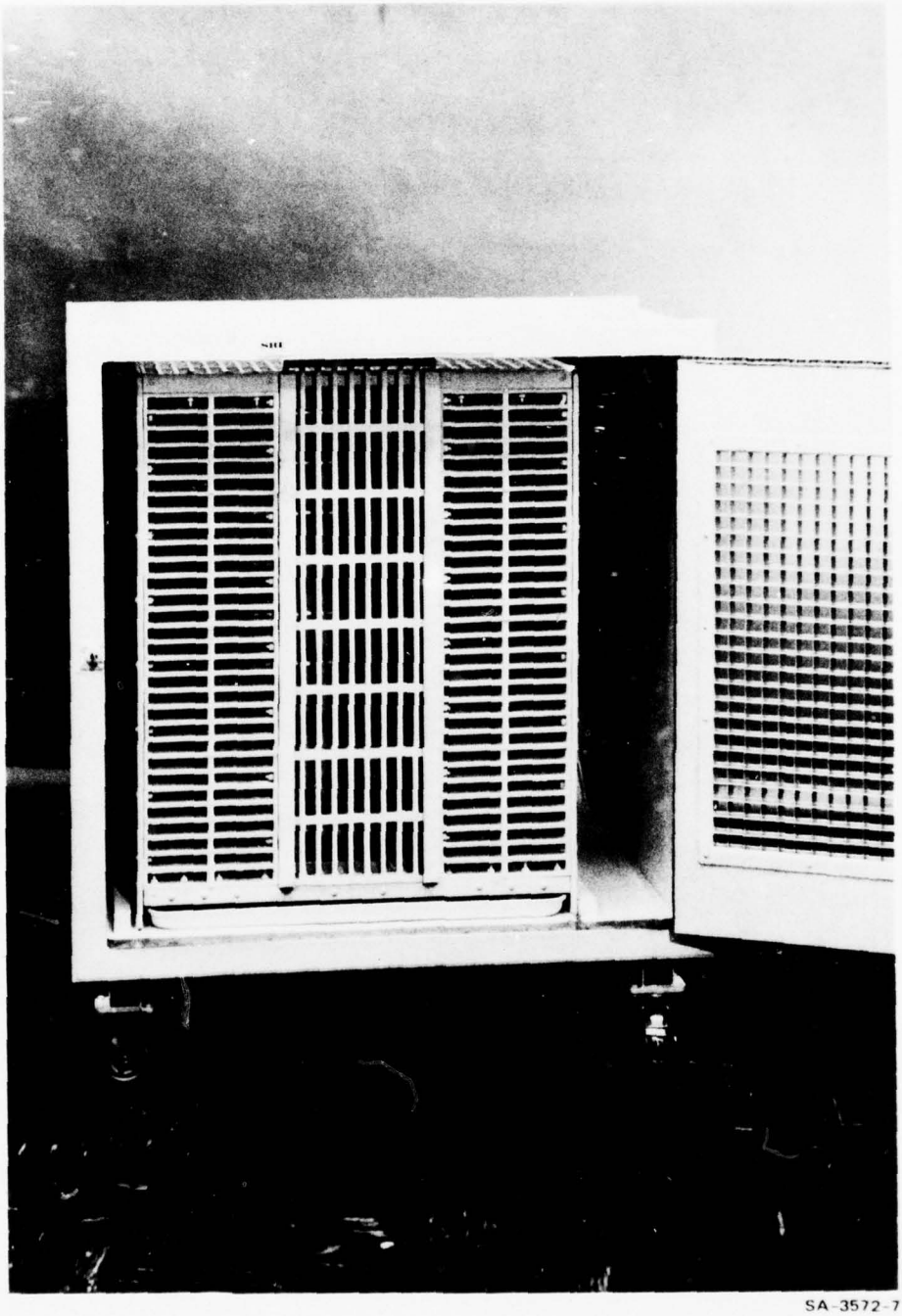

SA-3572-7

FIGURE 7 DIELECTRIC CAGE IN CAVITY

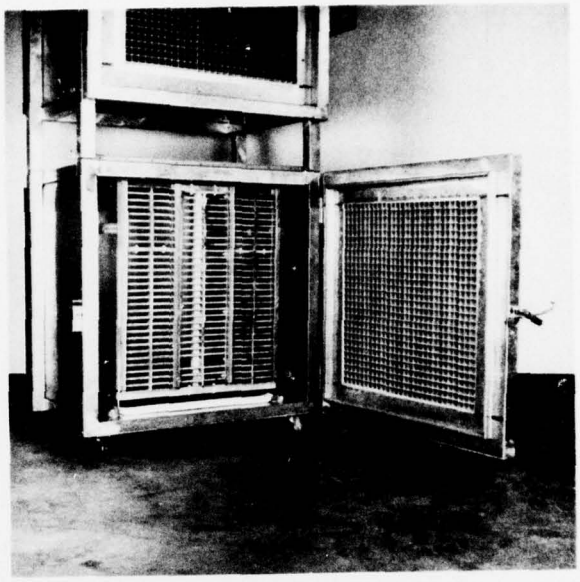

(a)

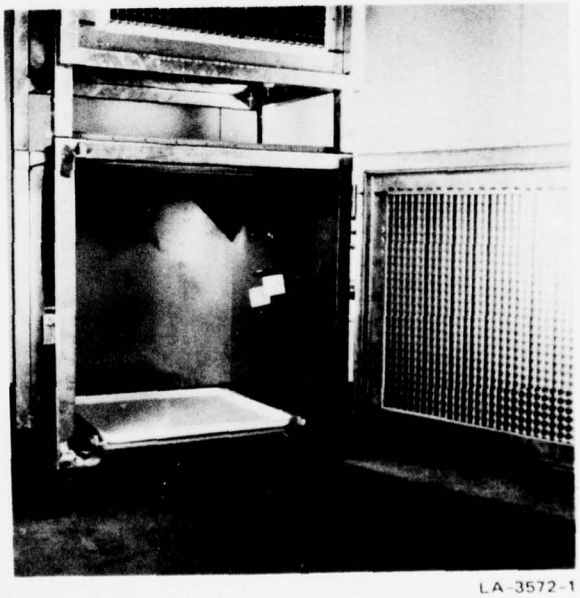

LA-3572-1

(b)

FIGURE 8 VERTICALLY STACKED PAIR OF IMPROVED CAVITY EXPOSURE MODULES; (a) WITH DIELECTRIC CAGES INSTALLED; (b) WITH CAGE REMOVED FROM CAVITY OF LOWER MODULE TO SHOW ADJUSTABLE IRIS, MODE STIRRER, AND ANIMAL WASTE-COLLECTION TRAY

needed whose output power could be varied over a wide and continuous range and yet be relatively inexpensive. Magnetrons fulfill these requirements well (hence, their wide usage in microwave ovens). After a number of helpful discussions with several manufacturers of microwave ovens, notably Litton (both in San Carlos and Minneapolis) and Gerling Moore (Palo Alto), we found it more economical to purchase a Litton Model 416 microwave oven and utilize many of its components than to buy the individual components separately.

The magnetron used in the Model 416 is a Type 2M53, which has an integral permanent magnet and operates at a cathode-to-anode voltage, V_{CA}, of approximately -4 kV (with anode grounded). Its performance chart, which is typical for inexpensive microwave oven magnetrons, is shown in Figure 9 for operation with unfiltered, full-wave-rectified ac. It is

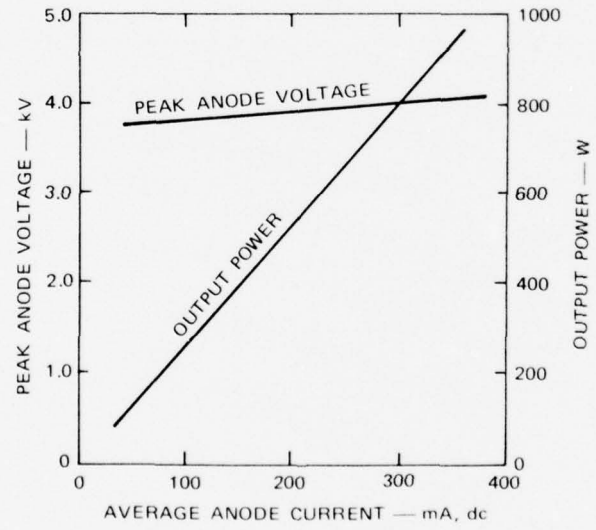

OPERATING CONDITIONS:

ANODE SUPPLY: SINGLE-PHASE, FULL-WAVE-RECTIFIED, WITHOUT FILTER
FILAMENT VOLTAGE: 3.15 V
LOAD VSWR: 1.1 MAX

SA-3572-10

FIGURE 9 TYPICAL PERFORMANCE DATA FOR TYPE 2M53 MAGNETRON

seen that almost the entire output-power range--i.e., 800 to 80 W--is obtained for only about a 5-percent variation (from 4.0 to 3.8 kV) of peak V_{CA} (called "anode voltage" in Figure 9); thus magnetron performance is very sensitive to the value of V_{CA}.

Under full-wave operation, the magnetron would be switched on and off each 60-Hz half cycle (i.e., 120 times per second) at the voltage points corresponding to the onset and cessation of oscillation. However, again primarily for economic reasons, the Litton Model 416 (as well as most microwave ovens for home use) utilizes a half-wave-doubler circuit--i.e., the magnetron is switched on and off only 60 times per second.

If a typical sinusoidal high-voltage transformer were used for either full-wave or half-wave operation, the instantaneous output power during the magnetron "on" periods would rise and fall sharply with the sinusoidal tops of the rectified half cycles because of the aforementioned sensitivity to V_{CA}, and would yield large peak-to-average output power ratios. For this reason the high-voltage transformers commonly used for microwave ovens are of the ferroresonant kind, designed to yield magnetic-field saturation at high current levels and thereby effectively "flatten" the sinusoidal tops to a significant degree. In this way, the variation of the instantaneous output power over each rectified half cycle is reduced considerably. Thus, in general, magnetron operation under either full-wave or half-wave rectification with a ferroresonant transformer yields a special form of modulated continuous-wave (CW) power, with a fundamental modulation frequency of 120 or 60 Hz, respectively.

We conducted operational tests to compare the half-wave-doubler-ferroresonant circuit removed from the Model 416 oven with a full-wave-doubler circuit, and discovered little, if any, technical superiority for the latter to warrant its adoption. Moreover, the components for the half-wave-doubler circuit are significantly less expensive (since they are

used in large numbers for home-use microwave ovens). Concurrently, we also considered magnetron operation with dc values of V_{CA} to obtain unmodulated CW. However, most magnetrons are not designed for dc operation and would be subject to the possibility of gradual electron emission buildup and runaway (i.e., at the end hats) if operated in this manner. (Special-purpose magnetrons having platinum end hats to minimize emission therefrom have been developed but are quite expensive.) In addition, we considered magnetron operation with multiphase power supplies (e.g., with a 12-phase, 60-Hz rectifier) and found it prohibitively expensive. Finally, we decided that from the viewpoint of thermal effects on tissues, operation under modulated CW conditions would differ insignificantly from unmodulated-CW operation because the thermal time constants of macroscopic tissues or organs such as the eye are much larger than the 1/60-second periods corresponding to 60-Hz modulated-CW operation. Consequently, we decided to use the ferroresonant half-wave-doubler circuit from the Model 416 oven. It should be emphasized, however, that we are aware that nonthermal biological effects from the use of modulated CW have been postulated, and that this point will be fully considered in analyzing the results to be obtained in subsequent phases of the cataractogenesis investigation.

2. RF Components

As indicated earlier, the unavailability of "off-the-shelf" components or the high cost of especially designed components in WR 340 waveguide size (internal transverse dimensions 3.40 by 1.70 inches) such as bidirectional couplers, ferrite circulators, bends, tees, and flexible sections, led us to adopt, provisionally, the WR 284 waveguide size (internal transverse dimensions 2.84 by 1.34 inches). Thus, the assembly of the WR 284 microwave components shown in Figure 10 was used for performing many of the tests with the prototype module. Butted directly to

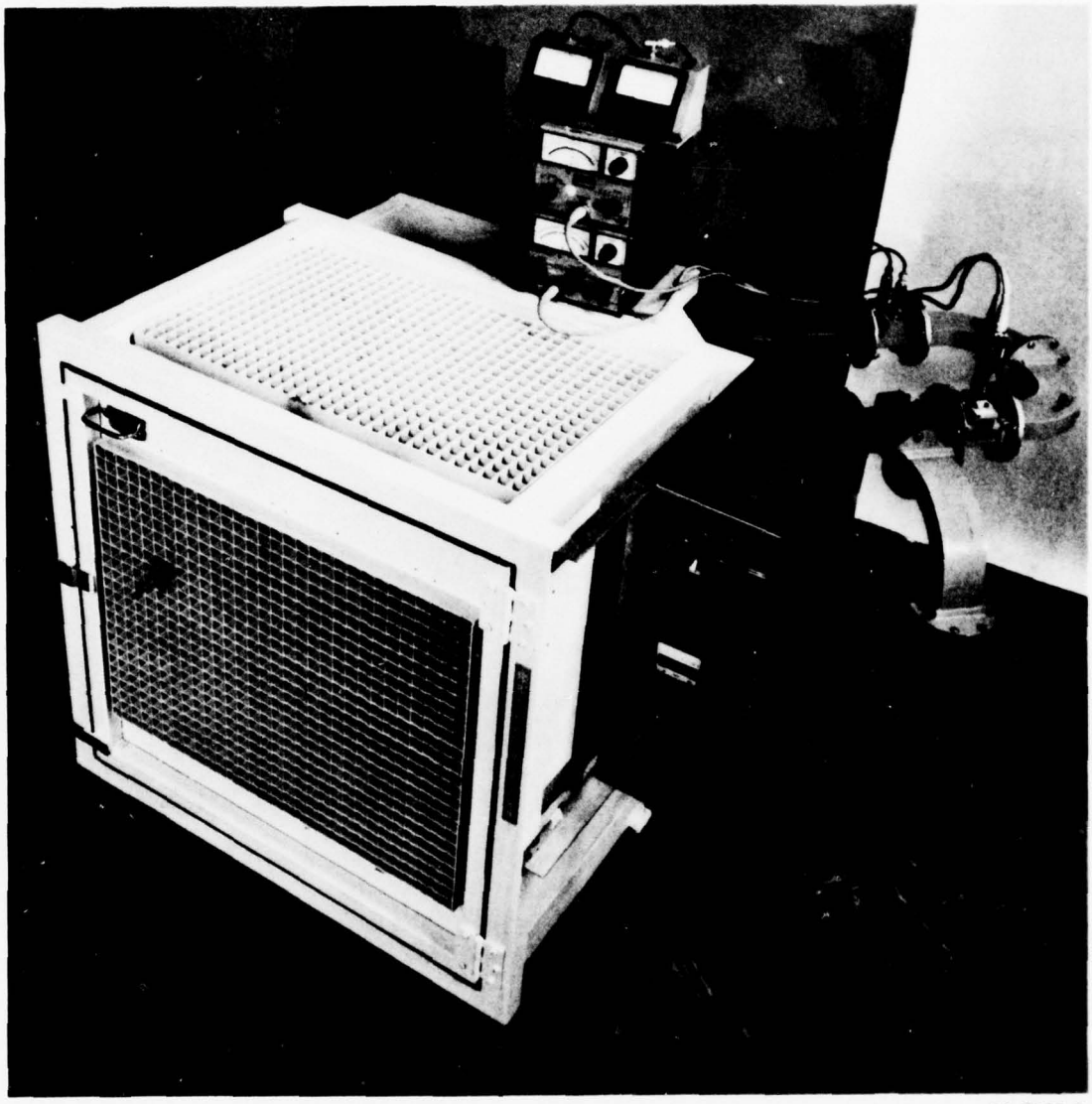

SA-3572-9

FIGURE 10 PHOTO OF MODULE WITH INTEGRAL MICROWAVE POWER UNIT

the magnetron waveguide launching section (which is not visible in this view but is discussed below) are: a Merrimac Industries Model FCW-1521 ferrite circulator with its side port terminated in a high-power RF load, a Gerling Moore bidirectional coupler, a U-shaped H-plane bend (two 90° bends butted together), another Gerling Moore bidirectional coupler, and a flexible section of waveguide that connects the second bidirectional coupler to the RF entrance of the cavity (through the adjustable iris).

Crystal detectors are connected to the auxiliary output ports of one of the bidirectional couplers for measuring forward and reflected power values when properly calibrated. The other bidirectional coupler proved useful in performing the calibrations, as described later.

In the Model 416 oven, the output probe (and surrounding glass dome) of the 2M53 magnetron is inserted in a WR 340 size waveguide launching section of proper design. We gave some consideration to designing a launching section in WR 284 size, but decided that it would be more economical in cost and time to utilize the larger WR 340 launching section from the oven and to fabricate a simple transition section between the two waveguide sizes. However, a simple RF test indicated that if the WR 340 launching section is merely butted directly to a section of WR 284 waveguide terminated in a matched load, the magnetron would "see" a VSWR value well below the maximum permitted by the magnetron specifications. Thus, no transition section was used in the prototype.

In subsequently producing the 12 modules for the EPA project, expensive commercial components such as the ferrite circulator, the two bidirectional couplers, and the high-power load were not used. Instead, it proved more economical to design and fabricate at SRI the necessary RF components in WR 340 waveguide size, including the bidirectional coupler, and to omit the circulator and load. Figure 11 shows the waveguide assembly of one of those modules.

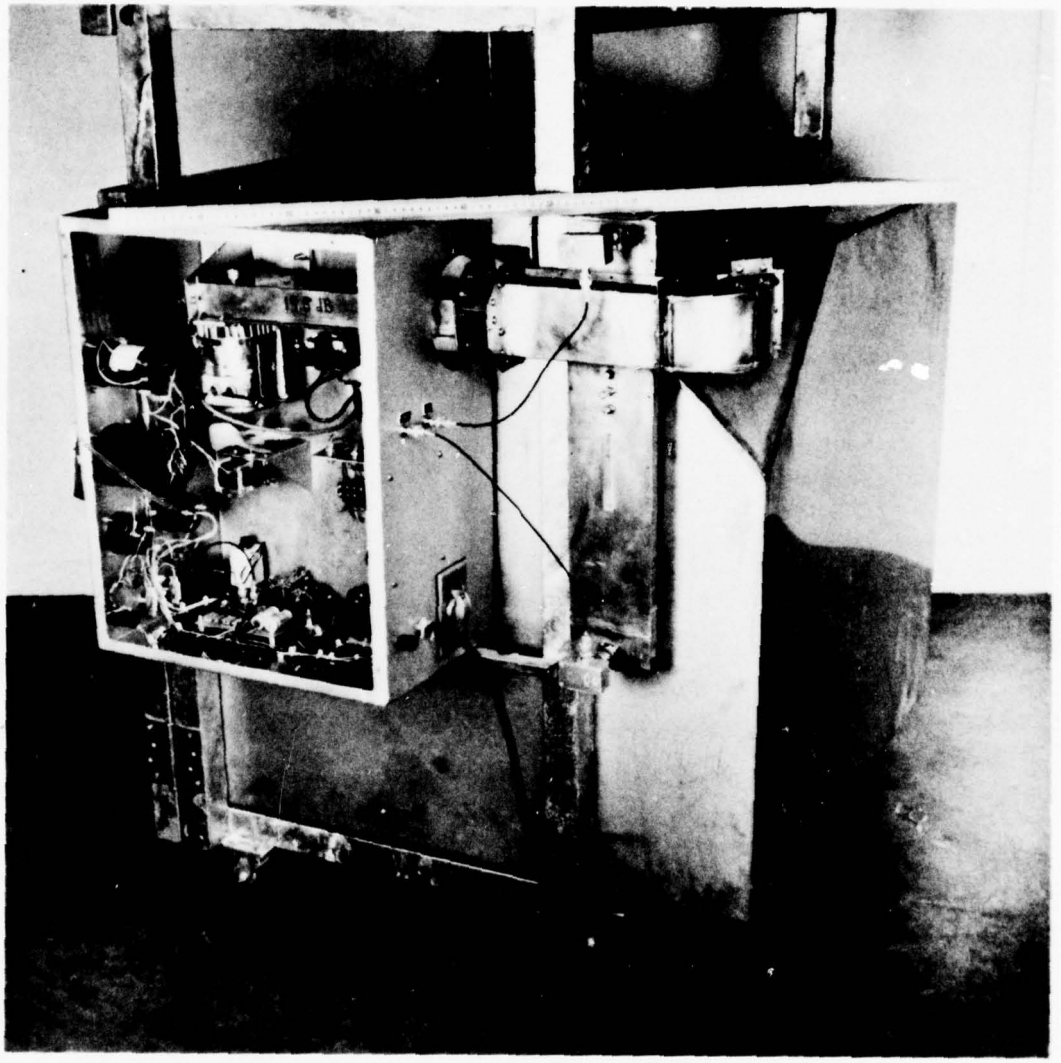

LA-3572-2

FIGURE 11 RF-DRIVE WAVEGUIDE ASSEMBLY AND CONTROL-CIRCUITRY BOX

3. Control Circuitry

The method implemented for setting the mean output power level of the magnetron to any desired value is phase-angle variation. Recall that with the half-wave-doubler power supply, the magnetron is turned on once during each 60-Hz period for a time interval somewhat shorter than half a period or 1/120 second. In the absence of any control circuitry, the mean RF power (per period) would constitute the full-power capabilities of the specific magnetron and power supply used. Phase-angle variation is a technique for shortening the duration of the "on" periods by any desired amount without significantly affecting the peak high voltage applied to the magnetron. In essence, the periods are shortened by delaying the time (increasing the phase angle) to the onset of magnetron oscillation. This technique permits setting the output power level to essentially any value within the range from full power to zero.

Another function required of the control circuitry is to hold constant the net power flow into the cavity and its contents after setting the phase-angle control to yield the desired level. This function is particularly important for investigations entailing irradiations of animals over long periods of time, because free movements of an animal within a unit, as well as spurious factors such as line-voltage variations, could otherwise alter the dose rate and total dose significantly.

Various circuits for implementing power-level setting by phase-angle adjustment have been devised, including inexpensive light dimmers for home use. However, incorporation of the power-holding function discussed above required the design of a special feedback circuit that would sense any change in the preset RF level and alter the phase-angle so as to restore the RF level. Our initial intent was to design a circuit that would form the difference between the output signals from the forward- and reflected-power crystal detectors on the bidirectional coupler and

apply this difference signal through a feedback loop to vary the phase angle so as to keep any preset net (forward minus reflected) RF power flow into the cavity constant. However, the RF loading of the cavity by the presence of the cage (both with and without bottles of saline water inside the cage) proved to be such that the reflected-power values never exceeded about 3 percent of the forward power; consequently, variations of reflected power could be ignored, with negligible error. Thus, in the control unit implemented, a detector signal proportional to only the forward-power level is used for feedback control.

A block diagram of the control unit devised is presented in Figure 12. The magnetron waveguide launching section is shown connected to the bidirectional coupler. The direct RF throughput port of the coupler feeds the cavity through the previously described adjustable iris. A Hewlett-Packard (HP) Type 420 crystal detector is connected, through a 10-dB coaxial pad, to the forward-power output port of the bidirectional coupler, and the output of the detector is fed to a 200 × gain operational amplifier, which in turn is connected to the forward-power indicator. This indicator consists of a 100-μA dc meter and an adjustable two-range resistor network for rendering the meter direct-reading at 1 kW and 100 W full-scale. The output signal of the operational amplifier is also fed to one input terminal of a 10 × gain difference amplifier, and an adjustable dc-reference voltage is applied to the other input terminal of the difference amplifier. Thus, the output signal from the difference amplifier is essentially proportional to the difference between the detected forward-power level and the reference level. This difference signal is fed to a Vectrol "Phasetrol" SCR Gate Driver Model VPH 5009-115-1A, thereby controlling the turn-on instant or phase angle (during each 60-Hz cycle) of a thyristor comprised of a pair of General Electric Type C230D silicon controlled rectifiers (SCRs). The SCRs are in series with the primary of the high-voltage transformer for the magnetron, so that this

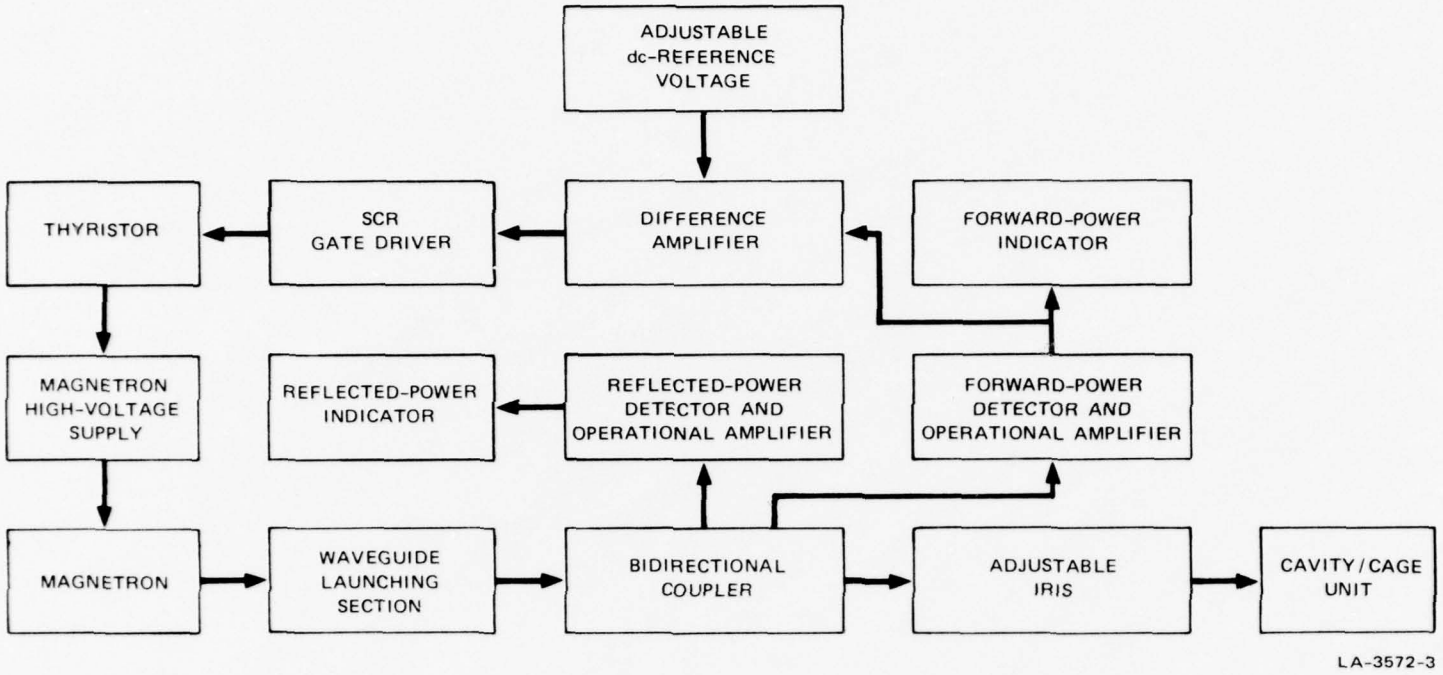

FIGURE 12 BLOCK DIAGRAM OF AN EXPOSURE MODULE

circuit controls the duration of the magnetron "on" periods, as discussed previously.

In operation, the dc-reference level is adjusted with a potentiometer, denoted the "Power Set" control, until the desired value of forward power is obtained, as indicated by the forward-power meter. Any subsequent spurious departure from this RF power value then results in a corresponding change in the output signal from the difference amplifier, automatically yielding a corrective adjustment of the phase-angle shift and hence a compensative change in the RF output of the magnetron.

The metering circuit for indicating reflected-power values is similar to that for forward-power readings but without the feedback loop. Thus, the required value of net power is obtained by adjusting the Power Set control so that the forward-power reading is higher than the net value by the amount indicated by the reflected-power meter.

The control circuitry box (with protective cover removed) of one of the EPA modules is shown in Figure 11. Figure 13 shows the control panel of this module. In addition to the forward- and reflected-power meters and the Power Set control, the panel includes: a timer to permit operation of the module for predetermined time periods that can be terminated by automatic shutoff; an elapsed-time meter to record cumulative operational duration; and the requisite switches and function-indicating lights for Power On, Standby (ac power on, but not RF), and Microwave Power On. The control circuitry also includes an automatic eight-second time-delay relay to allow the magnetron filament to warm up sufficiently prior to the application of the high voltage, and an interlock switch on the door of the cavity, mounted so that opening the door shuts off the magnetron power and operator action is required to restore power after the door has been reclosed.

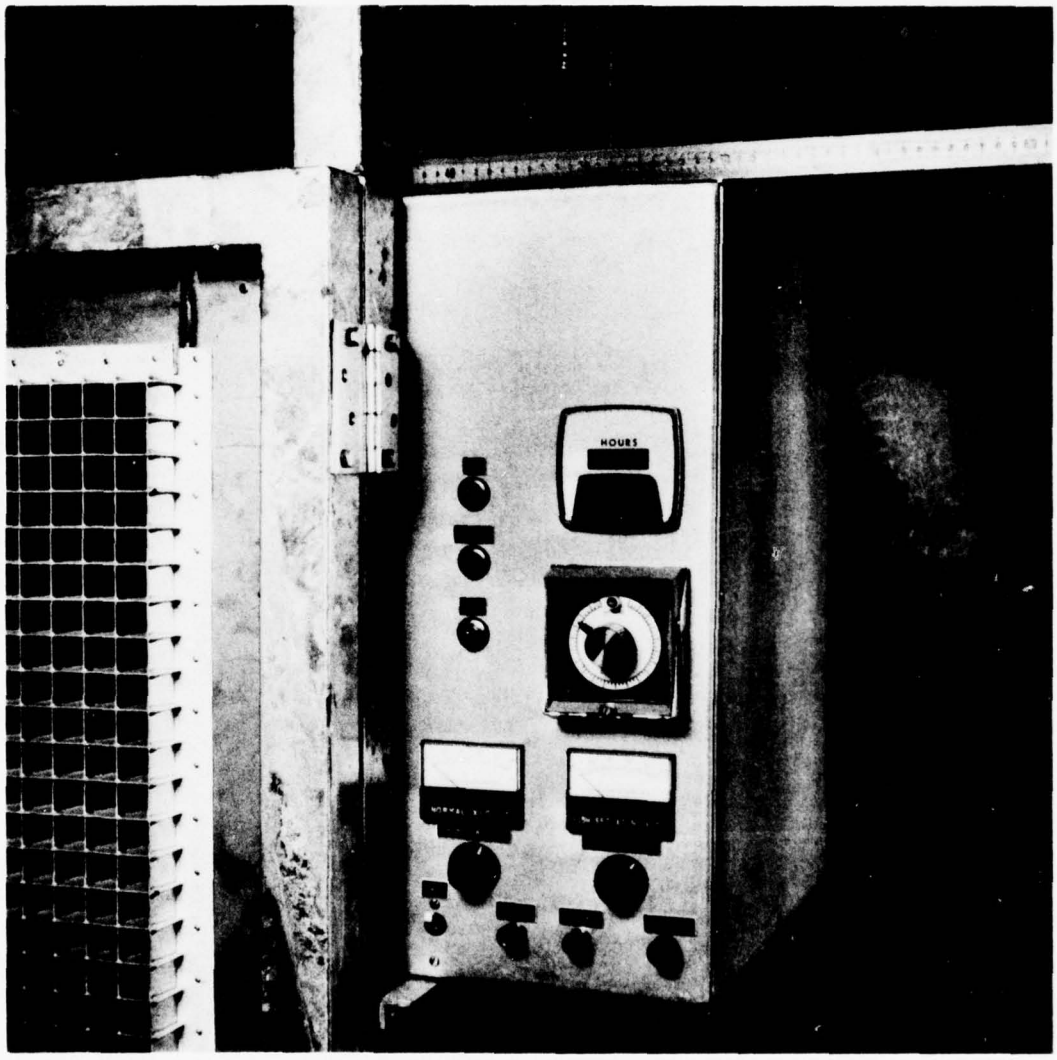

LA-3572-4

FIGURE 13 CONTROL PANEL OF AN EXPOSURE MODULE

4. RF Power Calibration Procedure

For economic reasons related to the costs of future modules, the decision was made early in the program to use crystal detectors at the auxiliary output ports of the bidirectional coupler for measuring forward and reflected powers, and to calibrate these detectors and associated metering circuits by using a precision RF power meter such as the HP Model 432 as the reference standard. A substitutional technique based on the use of two bidirectional couplers, as shown in Figure 10, proved convenient in calibrating the prototype module. One bidirectional coupler was purchased without crystal detectors or other RF power sensors to permit the use of an HP Model 432 power meter equipped with an HP Model 8478B bolometer; it will be called the "primary" coupler for the purposes of this discussion. The other bidirectional coupler, denoted the "secondary" coupler, was a unit removed temporarily from SRI's Gerling Moore Model 4003/4006 Microwave Power Source. It is similar to the primary coupler but has integral crystal detectors that had been calibrated in conjunction with the side-by-side pair of meters seen in Figure 10. First, the HP Type 420 crystal detector (and its metering circuit and feedback loop, described in the previous subsection) was disconnected from the forward-power output port of the primary coupler and the HP bolometer and power meter were substituted. Also, a digital voltmeter (DVM) was connected to the forward-power output port (integral crystal detector) of the secondary coupler. The RF power was set to predetermined "true" values as indicated on the 432 meter, and the corresponding readings of the DVM (in convenient arbitrary-scale units) were recorded. The HP 420 crystal detector and associated circuitry were then substituted for the bolometer and power meter, and the forward-power panel-meter reading corresponding to the DVM value was noted. This procedure permitted plotting a graph of panel-meter readings as a function of "true" forward-power values.

A similar technique was used for calibrating the reflected-power panel meter. However, with about 600 W of forward power fed into the cavity/cage unit, the reflected power did not exceed about 20 W. To obtain a calibration over the range from 0 to 100 W, recourse was had to removal of the cage, i.e., essentially unloading the cavity and thereby increasing the reflection coefficient.

D. Probe Measurements Within a Cavity

Early in the program we attempted to determine what variations of power density would be obtained at a fixed location relative to the surface of a bottle of saline water when the bottle is displaced to various positions within the cavity, under conditions of constant net power flow into the cavity. The values of the ratio of power density to net power flow would then provide a first approximation to the relationship between these two quantities, and the spatial variation of this ratio with bottle location would provide an initial assessment of dose-rate variation with position for a monkey.

For this purpose we had planned to mount a suitable (i.e., nonperturbing) RF probe at a fixed location on the bottle and to shift the assembly to appropriate locations within the cavity. However, we found that we were severely hampered by the lack of adequate commercial instrumentation. Although a Narda Model 8300 omnidirectional probe was available, we learned that such probes are equipped with nonperturbing high-resistance leads (60 kΩ/ft) that extend only 6-1/2 inches into the handle, as measured from the center of the sphere surrounding the sensor. At this point within the handle, the leads are joined to conventional conducting leads. Consequently, we could probe only a region within the cavity lying a short distance from the front radiopaque window. Therefore, we devised a relatively simple probe consisting of three mutually

perpendicular, thin-wire dipoles, each much shorter than a half wavelength and exciting a Type 1N4454 diode. The three diodes were connected in series (for dc purposes only) by high-resistance (20 kΩ/ft) leads,* and a long pair of the same kind of leads was used for connecting the ensemble to an external load of 2 MΩ, a value much higher than the remaining resistance in the circuit. Thus the rectified current generated by this RF sensor would yield a voltage output across the load that is virtually independent of the lead lengths. Also, since the currents flowing through the diodes would be very small, a square-law response would be assured.

The sensitivity and effective omnidirectionality of this probe were investigated by using the microwave field at the mouth of a waveguide horn having a taper from 2.84 by 1.34 inches to 8 by 6 inches at the mouth and excited at the narrow end with 2.45-GHz power. (The electric-field vectors at the mouth of such a horn are essentially parallel to the narrow dimensions.)

With the probe at a fixed angular orientation in the horn mouth, measurements of the output voltage across the 2-MΩ load versus the readings of the Narda 8300 meter over a suitable range of power levels yielded a substantially linear plot, indicating expected square-law operation of the diodes. However, the probe was found to have a significant degree of anisotropy--i.e., at a fixed power level, rotation of the probe (about its geometric center) yielded a ratio of about 1.6:1 between maximum and minimum readings. Nevertheless, after some minor improvements, we proceeded with the measurement of spatial variations of power density within the cavity. Although repeatable data were obtainable, the interpretation of such data proved difficult because of the presence of

---

*Carbon-impregnated Teflon, manufactured by Polypenco Division, Polymer Corporation, Reading, Pennsylvania.

multiple reflections between the bottle of water and the cavity walls and the changes in such multiple reflections with bottle position in the cavity. In fact, the results led us to question the validity of regarding dipole-probe measurements close to a surface as adequately representing the power density values at that surface. Therefore, this line of investigation was dropped, and the calorimetric measurements discussed below were performed.

E. Calorimetric Measurements

As was done in taking the probe measurements above, polyethylene bottles loaded with predetermined quantities (by weight) of 0.15 N NaCl solution were used as first approximations of the RF loads presented by monkeys. For convenience, the bottles used were cylindrical and of several radii, and the desired water height-to-radius ratios were obtained by filling the bottles to the requisite levels.

The calorimetric technique entailed measurements of water temperature with a rapid-response thermometer [a Yellow Springs Instruments (YSI) Model 42 SC Tele-Thermometer] immediately before and after driving the cavity with a specified value of net input power, P, for a specific time interval, t (equivalent to feeding a total energy $E = Pt$ into the cavity). Just prior to measuring water temperature (i.e., immediately before and after a power run), each bottle was agitated quickly to equilibrate its contents. To minimize thermal losses during the power runs, each bottle was enclosed entirely in 2-inch-thick styrofoam. The temperature rise, $\Delta\theta$, and the water mass, M_w, in each bottle were then used to calculate E_w, the energy absorbed by the water, and E_w/E, the fraction of the total input energy this constituted. The value of $P_w = E_w/t$ for each bottle of water used in any run was taken to represent its "whole-body absorption dose rate" for that run.

Although this calorimetric method cannot provide any information about variations of power density over the surface of a bottle of water, the use of bottles of simple geometry (e.g., cylindrical) permitted the calculation of the mean power density, F_w, defined by P/S ($= E_w/tS$), where S is the surface area of the water. Also, the ratio can be calculated for each value of water mass, M_w, to obtain estimates of the values of P required to obtain predetermined values of F_w.

For some of the calorimetric runs, particularly those performed during the earlier part of the program, the Gerling Moore Model 4003/4006 Microwave Power Source was used to drive the cavity. For the remainder of the runs, the integral 2M53 magnetron power source of the prototype module was used. Usually, the Gerling Moore unit was used to obtain power values of 1 kW and higher, and the integral magnetron unit was used for lower power values; in either case, the run durations were usually chosen to yield water temperature rises ($\Delta\theta$) of about 10°C or more. Thus, the experimental error of this calorimetric technique is estimated to be equivalent to about ±0.5°C in $\Delta\theta$ and hence about ±5 percent for $\Delta\theta$ values of 10°C or larger.

In some of the runs, single bottles were used; in others, two bottles constituted the load. In both types of runs, placement of the bottles was varied to assess the effect of load location and distribution within the module. The important results of all these runs are discussed below.

1. Runs Without Cage (Radiopague Windows Blocked)

Several initial runs were made without the cage installed, to eliminate any other possible RF power sink except the water bottles and the cavity losses. These runs were made with a single bottle of radius r = 7.6 cm containing 3.57 kg of saline water (i.e., filled to a height h = 19.7 cm). The bottle was placed at the center of the cavity, with

the base of the bottle eight inches above the cavity floor. The results were surprising in that only about 80 percent of the input energy was absorbed by the water, i.e., the cavity losses appeared to be much higher than expected. Leakage radiation through the radiopaque windows was hypothesized, but probing the outside of the windows with a Narda Microwave Radiation Monitor did not appear to yield any significant power transmission. However, it was soon discovered that the windows, particularly the top one, became quite warm to the touch during a run. (This fact was later confirmed by placing encapsulated liquid crystal sheets in contact with the windows.) The significant RF power absorption causing such heating was indicative of faulty window construction. As stated earlier, these windows are of 1-inch-square, 1-1/2-inch-deep brass grille, occupying areas 30 inches wide by 24 inches high in the door, and 30 inches by 18 inches in the top panel of the cavity. They were fabricated by cutting 3/4-inch-deep notches into 1-1/4-inch-wide brass strips at 1-inch intervals and assembling strips of proper length to form the grille. To ensure good RF contact at the corners of the squares, a nontoxic solder paste having a melting temperature of 430°F was brushed onto each joint and the grille was heated to 480°F for 30 minutes. However, from the results above, it was evident that this soldering process was unsatisfactory and that the windows would require repair. To provide base data for determining window quality after repair, we then blocked the windows temporarily with metal sheets and proceeded with the calorimetric runs.

Seven runs were made with the radiopaque windows blocked and with the cage not installed. For Run 1, a single bottle containing 3.57 kg of water was placed at the center of the cavity, 8 inches above the floor (as before), and 1.0 kW (net) was fed into the cavity for 5 minutes. Run 2 was similar except that a bottle containing the same quantity was placed at the same height near the left-front corner of the cavity (diagonally opposite the RF input--see Figure 5), and the bottle in the center

was removed. Run 3 was similar to Run 1 except for the use of 4.15 kg of water (a bottle of the same radius but filled to a height of 22.9 cm) and an input power of 0.9 kW. Run 4 was again similar to Run 1 except for the still larger quantity of water (4.36 kg, height 24.0 cm) and the higher input power (1.9 kW) used. In Runs 5 and 6, two bottles of the same radius, each containing 3.57 kg of water, were used to ascertain the effects of varying the spatial distribution of water. For Run 5, the two bottles were placed together at the center of the cavity at the same height and aligned approximately with the direction of the RF feed; in Run 6, the two bottles were widely spaced, one near the left front (diagonally opposite the RF input) and the other near the left rear of the cavity. Run 7 was similar to Run 5 except for the use of 4.15 kg of water in each bottle.

Table 1 shows the results of these seven runs, listed in order of increasing water mass. The values of the fractional energy, E_w/E, absorbed by the water indicate that the run-to-run variations were small and within the limits of the estimated experimental error. Nevertheless, we examined the data for trends but could not discern a definite or consistent dependence of these variations on water mass. Specifically, the variations of E_w/E with M_w were not monotonic for the single-bottle runs, for the two-bottle runs, or for both sets of runs considered as a single group. Also, there was no discernible relationship between E_w/E variations and bottle placement: Runs 1 and 2, differing only in the location of the single bottle used, yielded essentially the same value. In Run 5 with two bottles, Bottle A, which was closer to the RF input than Bottle B, exhibited a larger temperature rise and hence a larger value of E_w/E than Bottle B, whereas the converse was true for Bottles E and F in Run 7, which differed from Run 5 only in the quantity of water used. For all these reasons, we concluded that the run-to-run variations of E_w/E were essentially random. The mean value of E_w/E for these seven runs was 0.87

Table 1

CALORIMETRIC RUNS WITHOUT CAGE AND WITH BOTH RADIOPAQUE WINDOWS BLOCKED

Run No.*	M_w (kg)	P (kW)	t (s)	E (MJ)	$\Delta\theta$ (°C)	E_w (MJ)	E_w/E	S (cm^2)	F_w (W/cm^2)	P/F_w ($kW/W/cm^2$)	Conditions
1	3.57	1.0	300	0.30	18.0	0.27	0.90	1307	0.69	1.46	1 bottle; in center
2	3.57	1.0	300	0.30	18.0	0.27	0.90	1307	0.69	1.46	1 bottle; near left front
3	4.15	0.9	300	0.27	14.0	0.24	0.81	1462	0.55	1.81	1 bottle; in center
4	4.36	1.9	300	0.57	27.0	0.49	0.86	1518	1.08	1.76	1 bottle; in center
5	3.57(A)				9.0	0.13	0.45	1307	0.34	2.90	2 bottles together in
	3.57(B)				8.0	0.12	0.40	1307	0.31	3.27	center along diagonal;
	7.14(1)	1.0	300	0.30	8.5(2)	0.25(1)	0.85(1)	2614(1)	0.32(2)	3.09(2)	(A) nearer RF input
6	3.57(C)				9.5	0.14	0.47	1307	0.36	2.76	2 bottles; (C) near left
	3.57(D)				8.5	0.13	0.43	1307	0.32	3.09	front, (D) near left rear
	7.14(1)	1.0	300	0.30	9.0(2)	0.27(1)	0.90(1)	2614(1)	0.34(2)	2.92(2)	
7	4.15(E)				14.5	0.25	0.42	1462	0.29	3.48	2 bottles together in
	4.15(F)				15.5	0.27	0.45	1462	0.31	3.26	center along diagonal;
	8.30(1)	1.0	600	0.60	15.0(2)	0.52(1)	0.87(1)	2924(1)	0.30(2)	3.37(2)	(E) nearer RF input

*Not necessarily in chronological order of performance.

(1) Sum of values for run.

(2) Mean value for run.

with a standard deviation of 0.03. Insensitivity of E_w/E to water mass and bottle location would be expected when the water is the primary RF load within the cavity, which was true in each of these cases.

If the same value of input power were used in all the runs, then one would expect that the values of mean power density, F_w, would decrease with increasing water mass, M_w. Since the values of P used in Runs 3 and 4 were different from those used in the other runs, we normalized the values of F_w to their respective levels of P.

For cylindrical bottles, it is easy to show that the surface area, S, of the water within is given by

$$S = 2\pi r^2 + 2M_w/Dr \quad , \tag{1}$$

where D is the density of water (about 1 g/cm^3) and r is the radius of the cylinder. It then follows that the relationship between P/F_w (or F_w/P) and M_w is

$$\frac{P}{F_w} = \frac{E}{E_w}\left(2\pi r^2 + \frac{2M_w}{Dr}\right) \quad . \tag{2}$$

The second relationship shows that for constant values of E/E_w and for bottles of fixed radius, r (7.5 cm in these runs), P/F_w should be linearly related to M_w (where the range of M_w values is obtained by varying the height of the water in the bottle). A plot of the experimental values of P/F_w as a function of M_w for these seven runs is given in Figure 14 (circled points), through which a straight line can be passed, to within the experimental error. (It should be noted, however, that for variations of M_w by true scaling--i.e., by increasing all dimensions of the bottle by the same amount irrespective of its shape--P/F_w would vary as $M_w^{2/3}$.)

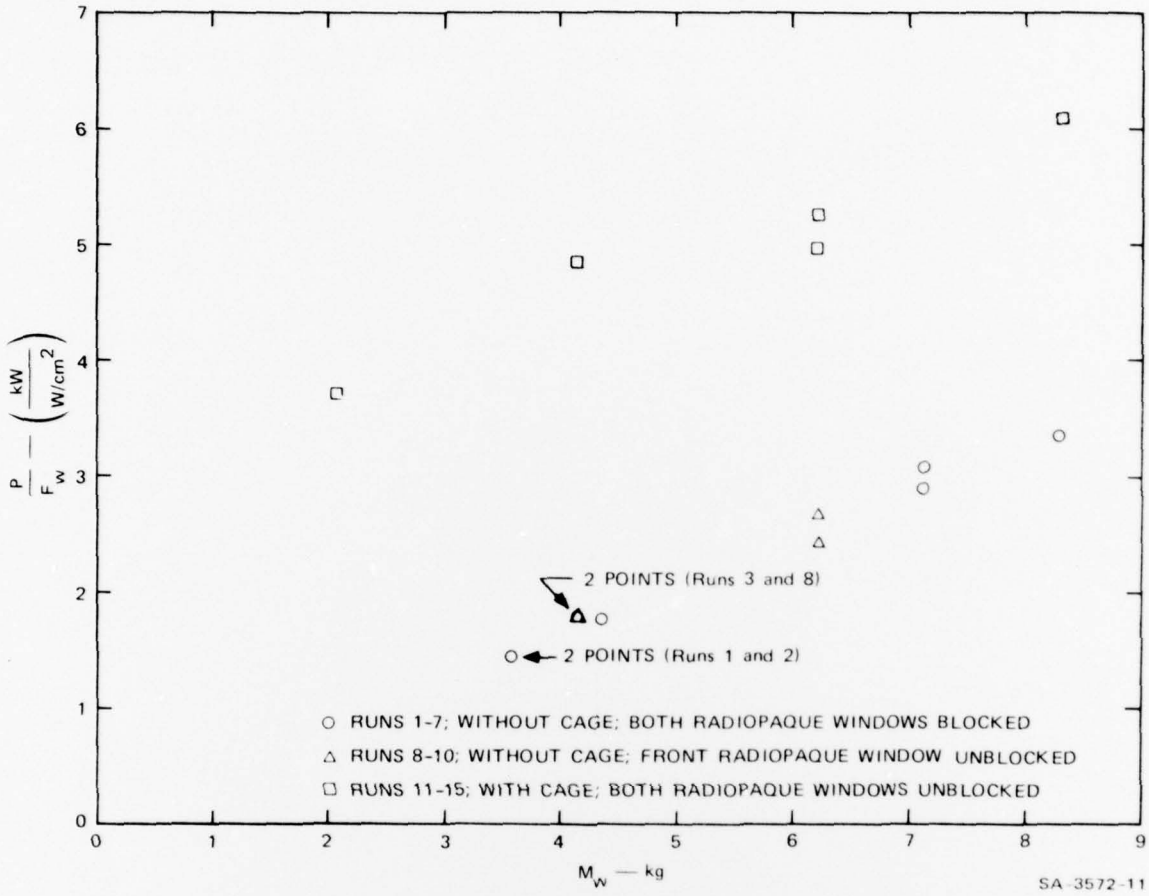

FIGURE 14 P/F_W AS A FUNCTION OF M_W

2. Runs Without Cage (Radiopaque Windows Unblocked)

Each radiopaque window was repaired by power sanding the grille along its inside plane (relative to the cavity) and soldering each intersection individually with rosin-core 60/40 (Sn/Pb) solder. We then made several runs without the cage installed, first with only the front window unblocked and then with both windows unblocked.

Table 2 shows the results for Runs 8, 9, and 10, taken with only the front window unblocked. Run 8 was similar to Run 3 (for which both windows were blocked) and the results were essentially the same.

Table 2

CALORIMETRIC RUNS WITHOUT CAGE AND WITH FRONT RADIOPAQUE WINDOW UNBLOCKED

Run No.	M_w (kg)	P (kW)	t (s)	E (MJ)	$\Delta\theta$ (°C)	E_w (MJ)	E_w/E	S (cm^2)	F_w (W/cm^2)	P/F_w ($kW/W/cm^2$)	Conditions
8	4.15	0.9	300	0.27	14.1	0.25	0.82	1462	0.56	1.79	1 bottle; in center
9	4.150(G)				19.7	0.34	0.57	1462	0.39	2.56	2 bottles together in
	2.075(H)	—	—	—	23.3	0.20	0.33	731	0.46	2.17	center along diagonal;
	6.225(1)	1.0	600	0.60	20.9(2)	0.54(1)	0.90(1)	2193(1)	0.41(2)	2.43(2)	(G) nearer RF input
10	4.150(K)				17.4	0.30	0.50	1462	0.34	2.90	2 bottles; (K) near
	2.075(L)	—	—	—	22.9	0.20	0.33	731	0.45	2.21	left rear, (L) near
	6.225(1)	1.0	600	0.60	19.2(2)	0.50(1)	0.83(1)	2193(1)	0.38(2)	2.67(2)	left front

(1) Sum of values for run.

(2) Mass-weighted mean value for run.

Also, the window remained cool, indicating that its repair was successful. Runs 9 and 10 were then performed to ascertain the effects of using two bottles, one having half the quantity of water in the other bottle. For Run 9 the bottles were placed in the center of the cavity along the RF feed-diagonal (as before), with the bottle having the larger amount of water (G) closer to the RF input. In Run 10 the two bottles were widely spaced, with the smaller bottle (L) near the left-front corner (diagonally opposite the RF input) and the larger bottle (K) near the left-rear corner. The values of P/F_w as a function of total water mass M_w for these three runs are shown as triangles in Figure 14. It is seen that these values are consistent with those from Runs 1 through 7. As expected, however, in Runs 9 and 10 the larger bottle absorbed the larger fraction of the input energy. There was some run-to-run difference in E_w/E value for the larger bottle (0.57 compared with 0.50), but it is difficult to ascribe any significance to this result, especially since the smaller bottle exhibited a negligible run-to-run difference.

The data obtained for the runs performed with both radiopaque windows unblocked (and without the cage installed) were deemed valueless and were discarded because of the subsequent discovery, along one of the boundaries of the top window, of a fine crack through which a significant power flow could be detected with a Narda probe. This crack was repaired, and we proceeded with the runs in progress with the cage installed. (It did not appear worthwhile to repeat the runs without the cage because during runs with the cage the top radiopaque window exhibited no significant temperature rise, indicating that its repair was also successful.)

It should be noted that this window problem with the prototype module was avoided in the 12 EPA modules by having the windows dip-brazed by an outside shop that specializes in such technology.

3. Runs with Cage Installed and Both Windows Unblocked

After fixing the aforementioned crack and ensuring that no other significant artifacts of a similar nature were present (by exploring the outer surfaces of the cavity with a Narda probe), we performed Runs 11 through 15 with the cage installed. The results are presented in Table 3, again in order of increasing water mass.

The first point to be noted is that the fraction of the energy absorbed by the water is relatively small, ranging from about 20 to 50 percent (compared with about 87 percent with the cage absent). Evidently the cage constitutes a relatively large RF load despite the fact that it is constructed from low-RF-loss materials. On reflection, this result can be accounted for qualitatively by the relatively large mass of the cage (about 40 kg) and the distribution of its mass over a large surface area because of its grille configuration. In essence, virtually all the cage mass is affected by the radiation because the cage is thinner (at all locations) than the skin depth at 2.45 GHz for the materials used.

Second, unlike the results for Runs 1 through 10, the fraction E_w/E of the input energy absorbed by the water is seen to increase with total water mass, which is also consistent with the presence of the large fixed RF load presented by the cage. If this consideration is included in a simple cylindrical-bottle model, then the relationship between P/F_w and M_w would not be linear but would exhibit a decreasing slope. This behavior can be discerned for the experimental values, shown as squares in Figure 14.

Third, comparison of the results for Runs 13 and 14, which were similar to one another except for bottle placement, shows that the larger bottle absorbed the greater fraction of the energy in each case (as with Runs 9 and 10), but that there was no significant difference ascribable to bottle placement within the module.

Table 3

CALORIMETRIC RUNS WITH CAGE INSTALLED AND BOTH RADIOPAQUE WINDOWS UNBLOCKED

Run No.	M_w (kg)	P (kW)	t (s)	E (MJ)	$\Delta\theta$ (°C)	E_w (MJ)	E_w/E	S (cm^2)	F_w (W/cm^2)	P/F_w ($kW/W/cm^2$)	Conditions
11	2.075	1.0	600	0.60	13.6	0.12	0.20	731	0.27	3.71	1 bottle; in center
12	4.15	1.0	300	0.30	5.2	0.090	0.30	1462	0.21	4.85	1 bottle; in center
13	4.150(M)				9.5	0.17	0.28	1462	0.19	5.31	2 bottles together in
	2.075(N)	—	—	—	11.8	0.10	0.17	731	0.23	4.28	center along diagonal;
	6.225(1)	1.0	600	0.60	10.3(2)	0.27(1)	0.45(1)	2193(1)	0.20(2)	4.97(2)	(M) nearer RF input
14	4.150(O)				9.0	0.16	0.26	1462	0.18	5.61	2 bottles; (O) near
	2.075(P)	—	—	—	11.1	0.096	0.16	731	0.22	4.55	left rear, (P) near
	6.225(1)	1.0	600	0.60	9.7(2)	0.26(1)	0.42(1)	2193(1)	0.19(2)	5.26(2)	left front
15	4.15(Q)				8.1	0.14	0.23	1462	0.16	6.23	2 bottles together in
	4.15(R)	—	—	—	8.5	0.15	0.25	1462	0.17	5.94	center along diagonal;
	8.30(1)	1.0	600	0.60	8.3(2)	0.29(1)	0.48(1)	2924(1)	0.16(2)	6.09(2)	(Q) nearer RF input

(1) Sum of values for run.

(2) Mass-weighted mean value for run.

Last, we found that a graph of P/F_w as a function of M_w can be useful for coarsely estimating the RF power requirements for future modules. To illustrate this point, suppose that the smallest monkey to be chronically irradiated at an F_w value of 10 mW/cm^2* has a weight of about 5 kg. From Figure 14, the corresponding value of P/F_w is approximately 5.2 kW per W/cm^2, which yields a value of 52 W for the net power required.

Regarding the relatively large RF load presented by the cage, we were concerned that the cage may become too warm during prolonged irradiation periods. Therefore, a run of about eight hours at an input power of 1 kW was made under normal room ventilation conditions with a representative saline-water load within the cavity/cage unit. At the end of the run, the cage was barely warm to the touch, indicating that excessive cage heating would not be a problem.

4. Summary of Calorimetric Work on Thermal Equivalence for Squirrel Monkeys†

As indicated in the footnote on p. 3, it is difficult to use biological endpoints as a basis for unambiguously defining power-density equivalence between cavity and unidirectionally incident plane-wave irradiation, and we therefore resorted to a form of thermal equivalence based on calorimetry. The specific objective was to determine, for plane-wave power densities of 10, 1, and 0.1 mW/cm^2, the corresponding

---

* For the purposes of this example, assume that this value of F_w is thermally equivalent, as defined in Section I, to 10 mW/cm^2 of unidirectionally incident plane-wave irradiation. In practice, the thermal equivalence relationship between the two forms of irradiation would be determined experimentally first, and the derived value of F_w corresponding to the desired plane-wave power density would then be used.

† Performed on Contract No. 68-02-2248 (SRI Project 4407) with the EPA. This summary is included in this report because of its relevance to the future use of such modules for cataractogenesis investigations.

values of power absorbed by each of two squirrel monkeys concurrently subjected to whole-body irradiation in one of the partitioned cavity/cage units, and to relate each power absorption value to the net power flow into the unit. Since performing calorimetry on actual squirrel monkeys was (and still is) not possible, we used cylinders containing 600 g and dolls containing 1000 g of 0.1 N NaCl solution. The dolls,* which had rubber skins about 2 mm thick, provided a better approximation to the geometry of squirrel monkeys; thus only the calorimetry results with the dolls are presented below.

To prevent heat loss from the dolls during the calorimetry runs, each was enclosed in a coffin-like insulating box constructed of 2-inch-thick styrofoam sheet. Immediately before and after the runs, the dolls were shaken vigorously and temperature measurements of the water were taken with the YSI Model 42 SC Tele-Thermometer.

Two identical dolls were used for the calorimetric work in the cavity/cage unit, one in each half of the partitioned cage. To check for possible regional variations of absorbed power within the cavity, we placed each doll in different relative positions and orientations within each half of the cage for each run and recorded the positions. In a representative series of 16 runs at a net power of 2.05 kW into the unit for two minutes, a mean temperature increase of 13.4 ± 2.06°C was obtained in each doll, corresponding to a linear temperature-rise rate of 6.7°C/min.. (The temperature variations from the mean, approximately ±15 percent, were caused primarily by the aforementioned changes in the relative positions and orientations of the two dolls.)

---

*This technique originally was used by A. Anne, "Scattering and Absorption of Microwaves by Dissipative Dielectric Objects: The Biological Significance and Hazards to Mankind." Doctoral Dissertation, University of Pennsylvania, Philadelphia, PA. NTIS Document No. AD-408997, 1963.

For the plane-wave calorimetry, one of the two dolls was irradiated in a 20 X 12 X 8-ft microwave anechoic chamber lined with Eccosorb* Type VHP-12 and CV-4 pyramidal microwave absorber. Microwave power from the Gerling-Moore Model 4003/4006 power source was fed into the chamber through a special sidewall manifold panel containing a WR 284 waveguide section. The waveguide was terminated in a flared, rectangular, unflanged, standard-gain feed horn. The E-field polarization was vertical. Forward and reflected microwave powers were measured using a bidirectional coupler, bolometers, and HP power meters (Type 432A for forward power and Type 431A for reflected power). The coupler previously had been calibrated accurately on an HP 8542B Automatic Network Analyzer. The doll (inside its styrofoam insulating box) was positioned vertically, facing the horn, 63.5 cm (25 inches) from its midplane to the face of the horn, with the center of the doll approximately collinear with the horn axis. Because this distance is greater than 5 wavelengths at 2.45 GHz, the doll was, for all intents and purposes, subjected to plane-wave radiation. A series of full-power experimental runs (approximately 1950-W net power flow to the feed horn) yielded a mean temperature rise in the doll of 12.86°C over a 15-minute exposure, corresponding to a temperature-rise rate of 0.857°C/min.

For these full-power runs, the power density at the location of the doll was too high to measure with a Narda Model 8300 Power Density Meter. By reducing the net power to the horn to bring the power density within the upper range of operation of the Narda meter, we could make a series of measurements of the net power fed to the horn corresponding to the power density at the location of the center of the doll in its absence. We then calculated, on a proportional basis, the power density

---

*Trademark of Emerson and Cuming, Inc., Waltham, Massachusetts.

for the calorimetric runs with the doll, and obtained the value 175 mW/cm^2 (for 0.857°C/min). Therefore, by proportionality again, a plane-wave power density of 10 mW/cm^2 would yield a temperature-rise rate of 4.90×10^{-2} °C/min.

Based on the 6.7°C/min value obtained in the cavity with 2.05 kW net power flow, a temperature-rise rate of 4.90×10^{-2} °C/min would require only 15 W of net power into the cavity unit. Thus, for a pair of saline-simulated, 1000-g squirrel monkeys, this net power value is taken to be the thermal equivalent of 10 mW/cm^2 of plane-wave radiation arriving frontally, full face, and with the E-vector parallel to the symmetry plane of the monkey's trunk. Similarly, the equivalents for 1.0 and 0.1 mW/cm^2 are 1.5 and 0.15 W, respectively.

IV CONCLUSIONS

The work described in Section III warrants the following conclusions:

(1) The primary objective of Phase I of this cataractogenesis investigation--the development and calibration of a prototype, RF-powered microwave cavity/cage system for chronically irradiating nonhuman primates as large as stumptail macaques--was achieved. This system embodies the following basic characteristics pertinent to investigations requiring chronic exposures of animals:

- The RF power input to the cavity and its contents (cage and animal) can be set to any predetermined value up to about 600 W (the upper limit determined by the type of magnetron used). Any preset value within the range is automatically maintained constant by a feedback loop.
- The radiation environment experienced by an animal within the cavity/cage unit is essentially omnidirectional and randomly polarized, because the large size of the cavity relative to the wavelength permits multimode, mode-stirred operation at 2.45 GHz. Therefore, the animal need not be constrained (other than confinement to its cage) during long periods of irradiation.
- Based on calorimetric work with saline-filled containers serving as first approximations of the RF loads presented by monkeys, the "whole-body" dose rate at a given input RF-power level is insensitive to location within the cage.
- Similar calorimetric work indicated, as expected, that at a fixed input level, the whole-body dose rate for an animal is inversely dependent on its weight. Therefore, in order to provide the desired dose rate, the input level must be selected accordingly.

(2) The subsequent construction of 12 modules based on the prototype and their use in chronic irradiation of squirrel monkeys for an EPA program entailed significant improvements in design and fabrication techniques. Because of this work, future modules can be built readily and economically.

(3) The thermal equivalence between plane-wave and cavity irradiation, determined calorimetrically for squirrel monkeys, is a useful concept that can be extended to other animals, particularly to the larger primates under consideration for this cataractogenesis program. However, concurrent infrared thermographic work is necessary to determine distributions of energy absorption and their relationship to the biological objectives of the program.

V RECOMMENDATIONS FOR FUTURE WORK

For the next phase of the cataractogenesis program, we recommend the pursuit of the following major aspects:

- Chronic irradiation of a group of animals at the plane-wave equivalent of 10 mW/cm^2 and concurrent sham irradiation of a group of control animals, both to be performed in cavity modules similar to those already constructed. Eye examinations of both groups of animals to be made by qualified ophthalmological consultants as frequently as is necessary during the irradiation regimen.
- Irradiation of groups of animals at power-density levels covering a suitable range above (and below, if necessary) the 10 mW/cm^2 value, to derive a relationship between power density and the time interval to the onset of eye damage, and to determine therefrom whether a threshold for eye damage exists.
- Postexposure examinations for latent effects over a suitable period of time, if the results of the tasks above indicate the importance of doing so.

In pursuing such a program, it would be very desirable to use a large number of animals, which would require a correspondingly large number of eye examinations as well as the construction, operation, and maintenance of the necessary modules. However, with due recognition to probable funding limitations, we have proposed, under separate cover, a minimal program that we believe would yield significant results.

ACKNOWLEDGMENTS

The assistance of the personnel listed below (in alphabetical order) in the design, construction, and testing of the prototype module is appreciated:

Eldon J. Fernandes	Engineering Assistant
Randall J. Logan	Design Engineer
Robert Segalla	Senior Technician

The advice and cooperation of Gerling Moore, Inc., Palo Alto, California, and of Litton Industries, San Carlos, California, on magnetrons and ancillary components are gratefully acknowledged.